




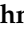


Review

# The Global Challenge of Fluoride Contamination: A Comprehensive Review of Removal Processes and Implications for Human Health and Ecosystems

Vivek Mariappan Santhi <sup>1,\*</sup>, Diwahar Periasamy <sup>2</sup>, Muthumari Perumal <sup>3</sup>, Prasanth Morkondan Sekar <sup>2</sup>, Varalakshmi Varatharajan <sup>3</sup>, Dhandapani Aravind <sup>4</sup>, Krishnasamy Senthilkumar <sup>5</sup>, Sundaresan Thirumalai Kumaran <sup>5</sup>, Saood Ali <sup>6,\*</sup>, Subramanipillai Sankar <sup>7</sup>, Nivetha Vijayakumar <sup>7</sup>, Charubala Boominathan <sup>7</sup> and Ragulasangeerthian Suresh Krishnan <sup>7</sup>

- <sup>1</sup> Department of Chemical Engineering, Indian Institute of Technology Madras, Chennai 600 036, Tamil Nadu, India
  - <sup>2</sup> Department of Plastic Technology, Central Institute of Petrochemicals Engineering & Technology, Chennai 600 032, Tamil Nadu, India; diwahar.aero28@gmail.com (D.P.); msprasanthmechanical@gmail.com (P.M.S.)
  - <sup>3</sup> Department of Biotechnology, P.S.R Engineering College, Sivakasi 626 140, Tamil Nadu, India; muthup2893@gmail.com (M.P.); varalakshmiotech@gmail.com (V.V.)
  - <sup>4</sup> University Science Instrumentation Centre, Madurai Kamaraj University, Madurai 625 021, Tamil Nadu, India; aravind.usic@mkuniversity.ac.in
  - <sup>5</sup> Department of Mechanical Engineering, PSG Institute of Technology and Applied Research, Coimbatore 641 062, Tamil Nadu, India; kmsenthilkumar@gmail.com (K.S.); thirumalaikumaran@yahoo.com (S.T.K.)
  - <sup>6</sup> School of Mechanical Engineering, Yeungnam University, 280, Daehak-ro, Gyeongsan 38541, Gyeongbuk, Republic of Korea
  - <sup>7</sup> Department of Chemical Engineering, Hindusthan College of Engineering and Technology, Coimbatore 641 032, Tamil Nadu, India; subramaniapillai2004@gmail.com (S.S.); nnive1835@gmail.com (N.V.); charubalaboomi01@gmail.com (C.B.); ragulasangeerthian5862@gmail.com (R.S.K.)
- \* Correspondence: ms.viv94@gmail.com (V.M.S.); saoodali@ynu.ac.kr (S.A.)



**Citation:** Mariappan Santhi, V.; Periasamy, D.; Perumal, M.; Sekar, P.M.; Varatharajan, V.; Aravind, D.; Senthilkumar, K.; Kumaran, S.T.; Ali, S.; Sankar, S.; et al. The Global Challenge of Fluoride Contamination: A Comprehensive Review of Removal Processes and Implications for Human Health and Ecosystems. *Sustainability* **2024**, *16*, 11056. <https://doi.org/10.3390/su162411056>

Academic Editor: Luca Stabile

Received: 8 October 2024

Revised: 2 December 2024

Accepted: 13 December 2024

Published: 17 December 2024



**Copyright:** © 2024 by the authors. Licensee MDPI, Basel, Switzerland. This article is an open access article distributed under the terms and conditions of the Creative Commons Attribution (CC BY) license (<https://creativecommons.org/licenses/by/4.0/>).

**Abstract:** Water resources are vital for humanity, but their quality has degraded in recent years due to increasing industrial activities. One significant issue is fluoride contamination, prevalent worldwide. Fluorides exist in combined states such as calcium fluoride, fluorapatite, and cryolite, originating from industrial processes like aluminum and fertilizer manufacturing. The World Health Organization warns against fluoride levels above 1.5 mg/L in drinking water due to health risks, including dental and skeletal fluorosis. Industrial activities also release fluoride-containing wastes into the environment, endangering ecosystems and human health. Overexposure to fluoride leads to disorders affecting organs including the kidneys, liver, and nervous system. Despite fluoride's benefits in controlled doses, excessive intake causes health problems, as evidenced by rising dental fluorosis cases in Brazil. Thus, effective and affordable fluoride removal strategies are crucial. Various methods exist, including adsorption, membrane technology, ion exchange process, electro dialysis, and electrocoagulation. Regulation of fluoride levels in drinking water is imperative to safeguard public health from its detrimental long-term effects.

**Keywords:** fluoride removal; adsorption; membrane technology; ion exchange process; electro dialysis; electrocoagulation

## 1. Introduction

Global climate change and the growing global population are increasing day by day, with the population expected to nearly double by 2050, and both are significantly linked to the increased need for water resources. Given that agriculture uses 70% of the world's

freshwater to generate food, there is a significant increase in the demand for freshwater. Worldwide Water Development 64 billion cubic meters of freshwater are reportedly utilized slowly each year, according to the World Water Development Report (WWDR). Water resources are one of the major resources of mankind. Freshwater resources on Earth are finite, and the pressures of worldwide industrial development are progressively degrading our water environments, leading to severe surface water pollution and pervasive eutrophication in lakes and reservoirs. The escalating population growth and rising living standards have imposed stringent drinking water quality standards. In recent years, water quality has dropped dramatically in regard to excess fluoride levels. The solute concentration in the water is rising due to certain industrial activities, i.e., such as the by-products of the manufacturing of aluminum, fertilizer, and iron ore [1]. Fluoride contamination in groundwater is now a major issue throughout the world. The fluorides remain in a combined state, such as  $\text{CaF}_2$  (calcium fluoride),  $\text{Ca}_5(\text{PO}_4)_3\text{F}$  (fluorapatite), and  $\text{Na}_3\text{AlF}_6$  (cryolite). Industrial waste, such as from the electronic and metal product sectors, is a source of fluoride. When these wastes dissolve into the soil, they pollute the groundwater. In contrast to groundwater, where the fluoride ion concentration typically exceeds 20 mg/L, surface water has a fluoride content of between 0.1 and 5 mg/L. Almost every place in the world has experienced problems with excessive fluoride levels in groundwater. For example, fluoride contamination at rates higher than 1.5 mg F/L has been identified in 30% of Tanzanian rivers, springs, and lakes. There is a broad distribution of exceptionally high levels of fluoride near Lake Momela, the summit of Mount Meru, and Kilimanjaro. It became known that Kenya's Lake Nakura has the greatest fluoride levels. The world's health organization (WHO) states that drinking water with a fluoride level greater than 1.5 mg/L is dangerous to humans, as reported in Table 1.

**Table 1.** Health impacts due to fluoride concentration in drinking water.

| Fluoride Concentration mg/L | Health Impact                 |
|-----------------------------|-------------------------------|
| <0.5                        | Dental decay in children      |
| 0.5–1.5                     | Strengthening of the skeleton |
| 1.5–4                       | Mottled enamel                |
| >6                          | Dental and Skeletal Fluorosis |
| >10                         | Crippling skeletal fluorosis  |

In coal, fluoride and chloride largely occur as inorganic chemicals that normally decompose into hydrogen fluoride (HF) and hydrogen chloride (HCl), along with some fly ash leftovers. After that, the desulfurization slurry absorbs the water-soluble hydrogen fluoride and hydrochloride with a greater than 95% efficiency even when fluoride concentrations are low, and since the levels of fluoride and chloride in coal are low, the desulfurization slurry's accumulated levels can reach up to tens of thousands of mg/L. The slurry is circulated to react with  $\text{SO}_2$  in a closed-loop ammonia-based FGD system. High levels of F prevent  $(\text{NH}_4)_2\text{SO}_4$  crystals from growing by adhering to their crystal faces, which lowers the product's quality and directly lowers the desulfurization efficiency. Fluoride can also seriously erode desulfurization equipment, with fluoride degrading silica-based materials and titanium alloys. In the previous 50 years, the United States has seen its worst droughts. As a result of soil erosion and soil runoff, water in water bodies above and below the ground is significantly more contaminated in nations with excessive rainfall. The increase in air and raw water temperatures in storage systems has a negative impact on the hygiene of the drinking water and leads to transmissible diseases. For instance, Legionnaire's disease can develop when legionella bacteria thrive in warm water at a temperature of 40 °C [2]. Due to its high-quality recovered water, water treatment plants in Singapore are a pillar for water sustainability strategy. Purified water is produced by treating wastewater before cleaning it with cutting-edge membrane technology and ultraviolet disinfection. It is completely harmless and free of risk.

According to reports, fluoride-containing slurries that are released into the environment without further treatment endanger local ecosystems. Overexposure to fluoride can result in serious disorders like dental and bone fluorosis. The soft tissues are also affected by the consumption of the highly concentrated fluoride in water, which is known as non-skeletal fluorosis [2]. High fluoride levels have been shown to cause metabolic damage to multiple organs. Including the kidneys, liver, endocrine glands, and the reproductive and nervous systems. A number of illnesses and health problems, including dental fluorosis, bone osteoporosis, intellectual disability, renal deficiency, and DNA changes, are associated with fluoride intake that exceeds the 1.5 mg/L tolerance level, according to the World Health Organization. While trace amounts of fluoride are beneficial for health, dental fluorosis has risen throughout Brazil from 2003 to 2010, reported by the Brazilian Oral Health Program (SBB). Dental fluorosis affects 53% of children under 12 in Santana, western Bahia, where rainwater from the Bambui aquifer underneath the city is regularly consumed. Thus, it is essential to develop strategies to remove excess fluoride that are both inexpensive and effective. Controlling the fluoride content in drinking water is essential since it has long-term detrimental effects on human health. Existing technologies like adsorption, coagulation, precipitation, and ion exchange have been widely employed for fluoride removal from natural water sources, but they fall short in consistently delivering high-quality water suitable for human consumption, particularly when addressing briny or saline groundwater. There are various standard methods for eliminating fluoride from water, notably adsorption, filtration utilizing membrane technology, precipitation, electrocoagulation, ion exchange, and electrodialysis [3].

## 2. Adsorption Technique

About 70% of people in dry North African countries and European nations lack adequate access to freshwater supplies. Innovative water purification and conservation technologies developed in the USA have shown how difficult it is to replenish depleted water reserves. Due to the immense pollution in the largest rivers and even their tributaries, more than 85% of China's main cities experience a water deficit. Utilization must be restricted to agricultural uses only. Schewe et al. [1] produced a multi-model analysis on the worldwide and regional shortages of freshwater driven on by climate change. Balaram et al. [2] reported it has been shown that a 2 °C increase in temperature beyond normal leads to a decline in the water supply by 15% across the world, raising the number of people who suffer from absolute water scarcity to close to 40%.

Typical cleaning processes, such as ozonation and chlorination, do not remove pollutants and may generate considerable levels of harmful by-products. The development of nanotechnology, which has inspired research and development in this sector, has aided in the growth of delicate, productive, and cutting-edge wastewater and water technologies. This review's main emphasis was on the characterization, performance, and applications of polymer brushes for water filtration. It also covered the membrane technique in relation to water filtration. The coexistence of arsenic and fluoride in natural waters is an important global problem. More severe health consequences on the neurological and circulatory systems may result from arsenic and fluoride exposure when they are combined than from either substance alone. Due to the inherent chemical variations between arsenic and fluoride, they exhibit various phenomena at the solid–water interface.

Simultaneous arsenic and fluoride removal has prompted a lot of research but has remained a difficult task. For small rural villages or single-family homes, adsorption is a feasible method of removing arsenic and fluoride. Because they are inexpensive and readily available, Fe-based adsorbents are a common adsorbent for the removal of arsenic and fluoride. Due to issues related to its poor regeneration and the safe treatment of the wasted media, Fe-based materials' advancement as an effective adsorbent may in some way be hampered. Due to its low cost and chemical stability, TiO<sub>2</sub>, an effective arsenic adsorbent, has recently attracted a lot of interest. The chemical element fluorine is widespread and highly reactive. Because it dissolves readily in water, it only appears

as fluoride in aqueous solutions. In accordance with US EPA regulations, the maximum amount of fluoride ions that can be released from wastewater treatment plants is 4 mg F/L. This limit was lowered to 0.7 mg F/L in some countries. Tanzania raised the acceptable level to 4 mg F/L in response to the primary cause of water contamination. Fluorine is able to reach the ecosystem from both natural and man-made sources. For example, the wastewater from the generation of phosphoric acid contains a quantity of fluoride that might exceed 3000 mg F/L. Fluoride is also released into the environment via the electroplating process, ceramics production, semiconductors development, domestic use, and the production of bricks and glass. Particularly, fluoride was removed by adsorption using various adsorbents, which are listed in Table 2.

**Table 2.** Adsorbent and process parameters for fluoride removal.

| S. No. | Adsorbent  | Concentration Range | pH         | Contact Time | Adsorption Range     | Reference |
|--------|--|---------------------|------------|--------------|----------------------|-----------|
| 1      | Lanthanum oxyhydroxides-anchored commercial granular activated carbon (GAC-La) | 1–80 mg/L           | 7 ± 0.2    | 40 min       | 9.98 mg/g            | [4]       |
| 2      | Single-walled carbon nanotubes (SWCNTs)  | 100 mg/L            | 6          | 45 min       | 50–150 mg/g          | [5]       |
| 3      | Hydroxyapatite-multi-walled carbon nanotubes (HA-MWCNTs)                       | 3–50 mg/L           | 3~8        | 3 h          | 30.22 mg/g           | [6]       |
| 4      | Akaganeite-anchored graphene oxide ( $\beta$ -FeOOH@GO)                        | 10–250 mg/L         | 2.1~10.4   | 60 min       | 17.67 mg/g           | [7]       |
| 5      | Zirconium-chitosan/graphene oxide (ZrCTS/GO)                                   | 13.42 mg/L          | 3~11       | 45 min       | 29.06 mg/g           | [8]       |
| 6      | Fe-impregnated chitosan (Fe-CTS)   | 10 mg/L             | –          | 6 h          | 1.97 mg/g            | [9]       |
| 7      | Zirconium-immobilized cross-linked chitosan (Zr-CCS)                           | 20–200 mg/L         | 6          | 40 min       | 48.26 mg/g           | [10]      |
| 8      | Hydrous zirconium oxide-impregnated chitosan beads                             | 9.7–369.2 mg/L      | 5          | 160 h        | 22.1 mg/g            | [11]      |
| 9      | La <sup>3+</sup> -modified synthetic resin@chitosan (CS@La-IDAMP)              | 20–30 mg/L          | neutral pH | 12 min       | 17.5 mg/g            | [12]      |
| 10     | La <sup>3+</sup> and mixed-rare earth magnetic chitosan beads                  | 5–25 mg/L           | 5          | 120 min      | 20.53 and 22.35 mg/g | [13]      |

### 2.1. Adsorbents

Adsorption has been identified as the most efficient way for removing fluoride among the different techniques in aquatic environments. This is due to its simple layout, low maintenance requirements, and scalable process. In recent years, various low-cost adsorbents have been utilized to remove the fluoride ion, including activated alumina, chemical resin, biochar, carbon nanotubes, fly ash, and other materials [14]. Adsorption can be carried out by using many adsorbents, but the adsorbents are mainly classified as the carbon based, chitosan and chitosan-modified adsorbents, natural minerals, metal materials, MOFs, biomaterials, LDHs, polymers, and resins for fluoride removal reported in Figure 1.

Adsorbents with bases in alumina and aluminum, calcium, metal oxides, or carbon are rapidly used to eliminate fluoride from water, as shown in Table 3. However, activated alumina is a well-established technique for fluoride removal; the adsorbent is somewhat expensive. Both the co-ion content (e.g., chloride, nitrate, or bicarbonate) that can reduce the adsorption capacity of the material (like alumina or modified alumina) by competing with fluoride for binding sites and the pH of the treated water have an impact on its performance [14]. Metal oxides have been impregnated into modified alumina in order to increase its fluoride sorption capacity. It is important to note that sorbents made of alumina and aluminum that are used to clean drinking water could be harmful to people's health because they leach neurotoxic aluminum.

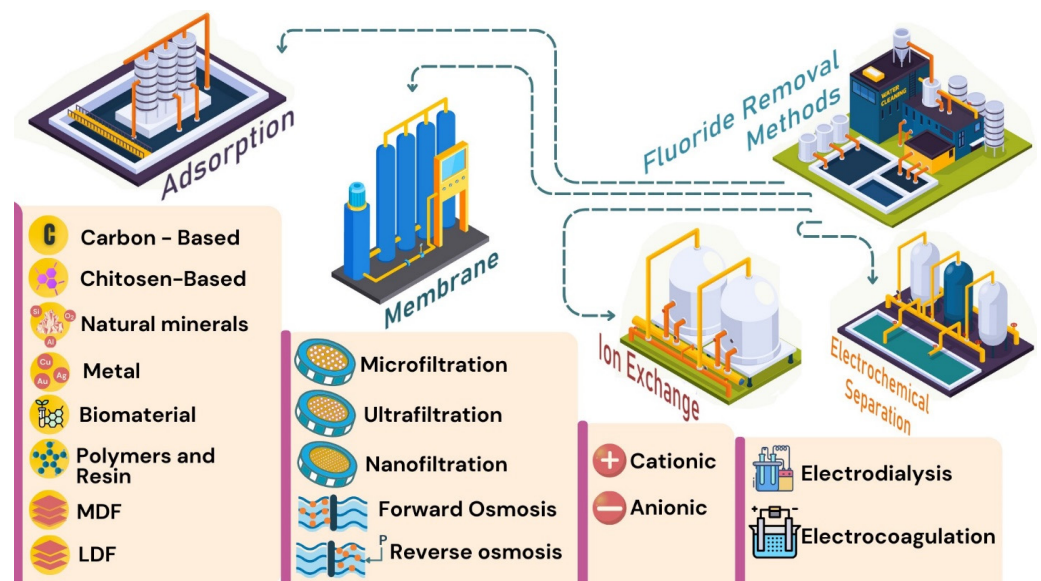


Figure 1. Utilization of adsorbents for the removal of fluoride.

Table 3. Adsorption isotherms and kinetic studies for fluoride removal by different adsorbents.

| S. No. | Adsorbent   | Isotherm Model  | Kinetic                    | Reference |
|--------|---|---|----------------------------|-----------|
| 1      | Single-walled carbon nanotubes                            | Langmuir isotherm                                       | second-order kinetic model | [5]       |
| 2      | Iron-impregnated chitosan granular                        | Langmuir  | pseudo-second-order model  | [9]       |
| 3      | Zirconium-immobilized cross-linked chitosan               | Langmuir  | pseudo-second-order model  | [10]      |
| 4      | Magnetic chitosan beads impregnated with $\text{La}^{3+}$ | Langmuir and Freundlich                                 | pseudo-second-order model  | [13]      |
| 5      | $\text{Mn}^{2+}$ -modified bentonite                      | Langmuir  | pseudo-second-order model  | [15]      |
| 6      | Novel $\text{CeO}_2/\text{SiO}_2$                         | Langmuir  | pseudo-second-order model  | [16]      |
| 7      | Zeolite   | Freundlich  | pseudo-second-order model  | [17]      |
| 8      | Bimetallic adsorbent                                      | Langmuir  | pseudo-second-order model  | [18]      |
| 9      | Titanium dioxide  | Langmuir and Freundlich (based on operating conditions) | pseudo-second-order        | [19]      |
| 10     | Metaettringite  | Freundlich  | pseudo-second-order model  | [20]      |

### 2.1.1. Carbon Based Materials

Carbon-based compounds with regulated pore frameworks and surface chemical compositions are utilized in many kinds of chemical reactions, such as adsorption. These materials are graphene-based compounds, activated carbon, carbon nanotubes, biochar, and graphite, which may be chemical adsorption processes as shown in Figure 2.

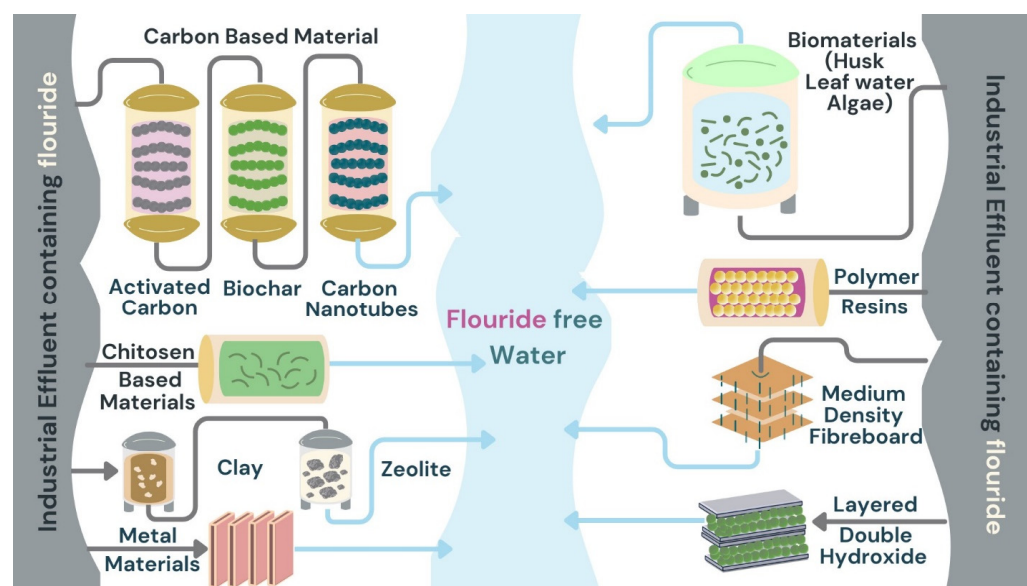
#### Activated Carbon

Activated carbon is known to be a powerful adsorbent because of its large surface area, high porosity, and intense enzymatic qualities [4]. Tests were conducted in which these activated carbon granules were dissolved with lanthanum oxyhydroxides to remove fluoride from water. According to the findings, the altered carbon adsorbent's potential to adsorb substances is significantly influenced by the concentration of lanthanum.

#### Biochar and Bone Char

Biochar is formed by the pyrolysis of biomass into energy. Since it is economical and readily accessible, it is often utilized as an adsorbing agent to remove fluoride from water [21,22]. Fluoride tests for adsorption were carried out on polypyrrole-grafted peanut

shells as the biological carbon. When 11.5 mg/L of fluoride solutions and 10 g/L of adsorbent were utilized, the modified adsorbent was found to have a 91.2% fluoride removal efficacy.



**Figure 2.** Adsorbents for fluoride removal.

#### Carbon Nanotubes

The experimental results were attributed to the second-order kinetic model and the Langmuir isotherm. It has been reported that single-walled carbon nanotubes (SWCNTs) with a particular surface area of  $712.9 \text{ m}^2/\text{g}$  as well as adsorption capacity ranging from 50 to 150 mg/g have a fluoride removal efficiency of around 87 to 100% at an initial concentration level of 100 mg per liter [5]. The innovative composite material composed of hydroxyapatite (HA) and multi-walled carbon nanotubes (MWCNTs) was produced using the in situ sol-gel technique that was previously used to remove fluoride from water. The defluoridation efficacy of HA-MWCNTs is 30.22 mg/g, and their specific surface area is  $180.504 \text{ m}^2/\text{g}$ . With a high effectiveness of 97.15%, synthesized HA-MWCNTs have the ability to reduce fluoride concentrations in real nuclear power plant effluent from 8.79 mg/L to around 0.25 mg/L [6].

#### Graphene and Graphite

Nanocomposites made of akaganeite and oxide ( $\text{FeOOH@GO}$ ) were created by Liu et al. [10]. The maximal adsorption capacity from the Langmuir isotherm was estimated to be 17.67 mg/g, and while the initial pH value varied from 2.1 to 10.4, it had little effect on the adsorption of fluoride [10]. Kuang et al. [7] investigated the influence of crystalline structure formation produced by acetate sodium on  $\text{FeOOH@GO}$  and revealed that organic ligands such as acetate substantially altered the crystalline structure of  $\text{FeOOH}$ , impacting the fluoride adsorption process and efficacy. When the pH range was 2.1 to 10.4,  $\text{FeOOH} + \text{Ac}/\text{GO}$  had an adsorption capacity of 19.82 mg/g, which was greater than  $\text{FeOOH}/\text{GO}$  (17.65 mg/L, pH 2.8–10.4). Zirconium chitosan/graphene oxide (Zr-CTS/GO) membranes were developed by Zhang et al. [8] to eliminate the fluoride from aqueous solutions. The two-site Langmuir model indicated that it would have an adsorption capacity of 26.06 mg/g. It was also demonstrated that fluoride adsorption occurred on the outside surfaces of multilayer heterogeneous Zr-CTS/GO membranes through a significant correlation between the isotherm data and the Freundlich model [10].

### 2.1.2. Chitosan and Chitosan Modified Adsorbents

Chitin poly- $\beta$ (1-4)-2-acetamide-2-deoxy-D-glucopyranose is partially or completely N-deacetylated to yield chitosan. Because of its short ion radius, substantial electronegativity, and intense attraction to positively charged multivalent metal ions—such as those of transition and metallic rare earths such as Al (III), Fe (III), Ti (IV), La (III), Zr (IV), Ce (III), and more—the fluoride ion is recognized as a strong base. Numerous studies have investigated the incorporation of the above metal ions into chitosan to increase adsorption capacity while simultaneously decreasing adsorbent costs.

Zhang et al. [9] evaluated the usage of an iron-impregnated chitosan granular adsorbent (Fe-CTS) for eliminating fluoride in aqueous solutions, achieving an adsorption capacity of 1.97 mg/g at a fluoride concentration of 10 mg/L. In another investigation, Liu et al. [10] used zirconium-immobilized cross-linked chitosan (Zr-CCS) as a fluoride adsorbent. Applying the Langmuir isotherm approach, they found a maximum adsorption capacity for fluoride of 48.26 mg/g. Cho et al. [11] synthesized a composite adsorbent by mixing hydrous zirconium oxide (HZrO) with chitosan in a 1:1 mass ratio. Their research revealed that a combination of sorbate systems outperformed the single-sorbate method for fluoride adsorption, with an optimal adsorption capacity of 22.10 mg/g.

Prabhu et al. [12] used an innovative approach to further investigate the formation of lanthanum complexes on an iminodiacetic acid and chitosan composite (CS@La-IDAMP) for effective fluoride adsorption. Liang et al. [13] synthesized magnetic chitosan beads loaded with  $\text{La}^{3+}$  and a rare earth element combination (MCLB and MCLRB). They discovered the following sequence of the influence of existing anions on fluoride adsorption through their experiments:  $\text{CO}_3^{2-} > \text{HCO}_3^- > \text{SO}_4^{2-} > \text{NO}_3^- > \text{Cl}^-$ . The adsorption capabilities of MCLB and MCLRB were 20.53 mg/g and 22.35 mg/g.

### 2.1.3. Natural Minerals

Natural minerals are characterized as individual natural substances or compounds that originated through geological processes and maintain a relatively consistent chemical composition. In the context of pollution prevention and environmental restoration, natural minerals hold a unique significance due to their distinct advantages in terms of scope, cost-effectiveness, efficiency, and environmental impact in pollution management. This research categorizes the natural minerals employed for fluoride removal into the following groups: calcium-based minerals, clay, zeolite, silica, and other mineral types.

#### Clay

Clay is composed primarily of various hydrated silicates, along with trace amounts of alkali metal oxides, aluminum oxide, and alkaline earth metal oxides. It boasts a substantial specific surface area and features negatively charged particles, which impart robust surface chemical reactivity and physical adsorption capabilities, enabling cation exchange. A range of clay materials, including polygorskite, various clay minerals, kaolinite, diatomite, vermiculite, bentonite, and others, are under evaluation for their capacity to remove fluoride, both in their natural and modified forms.

Ben Amor et al. [23] analyzed the defluoridation of water with natural Tunisian clays. They found that at an initial fluoride content of 2 mg/L, smectite and kaolinite removed 46% and 73% of the fluoride, respectively. Zhang et al. [24] employed naturally occurring clay modified with lanthanum and aluminum for the purpose of defluoridation. They observed that the adsorption capacity of this material was measured at 1.30 mg/g. Moreover, Mudzielwana et al. [15] coated Na-activated bentonite with  $\text{MnO}_2$  (known as Mn-NaB) using an in situ reduction method including  $\text{KMnO}_4$  to effectively create an effective fluoride adsorbent. Even while Mn-NaB's adsorption capacity of 2.40 mg/g was found to be lower than that of other types of adsorbents, its fluoride adsorption rate was remarkable, obtaining a 91% elimination rate throughout an extensive pH range of 2 to 12.

## SiO<sub>2</sub>

Izuka et al. [20] investigated the potential of diatomite for water defluoridation. Diatomite, predominantly composed of silica at 83.1%, with a minor presence of Al<sub>2</sub>O<sub>3</sub>, was the subject of their study. When examining a solution initially containing 100 mg/L of fluoride, they determined the optimal adsorption capacity to be 5.79 mg/g. Under these optimal conditions, only 25.62% of the maximum fluoride content could be effectively removed. Furthermore, the researchers examined diatomite as a modification utilizing Al/Fe oxides, obtaining an excellent maximal fluoride adsorption effectiveness of 93.1% with a dose of 0.6 g/100 mL over a 50 min treatment of a 10 mg/L fluoride mixture. Under these circumstances, the adsorption capacity of a mixture with 100 mg/L of fluoride attained 7.63 mg/g. Another notable adsorbent is mesoporous silica. Its substantial surface area and effective dispersion, particularly when modified with lanthanum, contribute to its efficacy in defluoridation. Under optimal conditions, fluoride removal rates can approach 90%, with a maximum adsorption capacity of 19.85 mg/g [25]. Zhang et al. [26] used cerium to modify mesoporous silica. The Langmuir adsorption isotherm plays a crucial role in fluoride removal from water as it assumes monolayer adsorption on a homogeneous surface, optimizing adsorption efficiency. It is widely applicable to various adsorbents like SWCNTs, iron-impregnated chitosan, and zirconium-based materials, demonstrating high specificity and capacity for fluoride ions. The Langmuir isotherm adsorption model adequately represented the fluoride ion adsorption process of Ms-Ce, according to the isothermal adsorption findings. Ms-Ce has the maximum achievable adsorption capacity of 17.96 mg/g. In contrast to several previously reported adsorbents, Wang et al. [27] introduced a novel CeO<sub>2</sub> SiO<sub>2</sub> adsorbent that achieved significantly greater adsorption efficiency, ranging from 257.70 to 363.90 mg/g, when employed for adsorbing fluoride ions from wastewater.

## Zeolite

Zeolite, characterized by its favorable ion exchange and adsorption properties, is a water-bearing aluminosilicate mineral containing alkali or alkaline earth metals. However, zeolites possess negative charges across all pH values, resulting in a high adsorption capacity for cations but a lower adsorption rate for anions due to electrostatic repulsion. Balarak et al. [28] conducted the synthesis of nano-sodalite zeolite through hydrothermal crystallization. This nano-sodalite zeolite adsorbent demonstrated excellent performance in removing fluoride. With a maximum adsorption capacity of 25.44 mg/g at 298 K, the equilibrium data were successfully predicted using the Langmuir model. Tian and Gan used nanohalloysite and NaOH to generate a three-dimensional, hierarchically arranged zeolite. This zeolite revealed significant fluoride adsorption capacities of up to 161 mg/g for fluoride ions. Saucedo-Delgado et al. [29] employed thermochemical treatment with NH<sub>4</sub>Cl to generate protonated clinoptilolite with a substantial specific surface area. This adsorbent excelled with both unmodified and modified zeolites, including multivalent cations like aluminum or iron.

## Calcium-Based Materials

These minerals primarily consist of apatite, limestone, and brushite. Apatite, a calcium-containing phosphate mineral, is usually recognized as hydroxyapatite (HAP). He et al. [30] successfully synthesized ultra-long HAP nanowires. These nanowires exhibited an adsorption capacity of 40.65 mg/g once exposed to a fluoride concentration of 200 mg/L. Through a suction filtration process, the HAP nanowires were transformed into membranes, enabling efficient fluoride removal via continuous filtration. Furthermore, they pointed out that calcium-based minerals are readily available and cost-effective materials that may not be highly effective as adsorbents for fluoride removal in their natural state. However, when subjected to physical and chemical modifications, their fluoride adsorption capacity can be significantly enhanced, making them suitable for practical applications. In another study, Mehta et al. [31] produced HAP nanorods using both conventional and ultrasonic



precipitation methods. The outcomes showed that the yield of HAP obtained through these methods was higher. These HAP nanorods achieved an impressive fluoride removal efficiency of 93%.

#### Other Minerals

Jia et al. [32] employed a simple hydrothermal method to synthesize bayerite/boehmite nanocomposites. These nanocomposites exhibited outstanding adsorption properties for fluoride, demonstrating an adsorption capacity of 56.80 mg/g at a pH of 7.0. In another study, Zhang et al. [33] developed a hydrothermal palygorskite composite loaded with lanthanum and aluminum (La-Al-HP) simulated groundwater. The composite achieved an adsorption capacity of 1.30 mg/g. The presence of  $\text{La}^{3+}$  and  $\text{Al}^{3+}$  elements, known for their strong affinity for fluoride ions, significantly enhanced the adsorption rate of hydrothermal palygorskite. Furthermore, Zhu et al. [34] manufactured natroalunite microtubes through a straightforward hydrothermal process, resulting in a notable surface area of 206.25 m<sup>2</sup>/g. These microtubes displayed an impressive maximum adsorption capacity of 85.84 mg/g for fluoride.

#### 2.1.4. Metal Materials

Fluoride ions exhibit a strong attraction to multivalent metal oxides due to the smaller ion size and high electronegativity of these metals, qualities that are advantageous for effective fluoride adsorption. Fluoride adsorbents based on metals can be categorized into the following three groups: single metal, binary metal, and ternary metal.

##### Single Metal

Ali et al. [35] produced a nano-impregnated adsorbent using green technology, and at an adsorbent dose of 2.5 g/L and an initial fluoride content of 4.0 mg/L, they were able to obtain a maximum fluoride removal rate of up to 90%. Moreover, the percentage of fluoride removed varied from 90% to 100% when this adsorbent was used for fluoride adsorption in natural groundwater. By using a wet-chemical precipitation technique followed by ethanol processing, Zhang et al. [36] created an iron oxide adsorbent. The ethanol treatment prevented crystallization and modified the adsorbent's microstructure. Consequently, the ethanol-treated adsorbent showed a high adsorption rate and a rise in fluoride adsorption capacity from 10.90 to 62.30 mg/g. Kumari et al. [37] investigated the impact of acid activation on the fluoride removal capacity of alumina. Alumina demonstrated a fluoride removal capacity of 96.72% with acid activation, compared to 63.58% without acid activation. Additionally, they synthesized a novel adsorbent through a straightforward process involving the nitric acid activation of alumina.

##### Two Metals

Zhu et al. [38] employed a precipitation and calcination method to fabricate a binary oxide composed of Al (III) and Zr (IV), referred to as  $\text{Al}_2\text{O}_3\text{-ZrO}_2$ . This adsorbent harnessed the advantageous properties of both  $\text{Al}_2\text{O}_3$  and  $\text{ZrO}_2$ , resulting in a remarkable maximum adsorption capacity of 114.54 mg/g. Yu et al. [39] produced a composite material known as  $\text{TiO}_2\text{-ZrO}_2$ . Their research findings highlighted the effectiveness of  $\text{TiO}_2\text{-ZrO}_2$  in concurrently removing fluoride and arsenic, and it exhibited favorable characteristics for regeneration and practical application. Meanwhile, Tao et al. [40] chose Ce-AlOOH as their adsorbent, recognizing that the addition of cerium (62.80) could significantly enhance the adsorption capacity, ultimately reaching 90 mg/g.

##### Three Metals

Chi et al. [41] generated a trimetallic composite adsorbent consisting of Mg-Al-Ce with a maximum adsorption capacity of 124.89 mg/g. Wang et al. [42] produced a triple metal composite, Mg-Al-Zr, with a defluoridation capacity of 22.90 mg/g in another study. Yu et al. [43] utilized co-precipitation to produce a Fe-Mg-La triple metal composite with a

notable highest capacity for adsorption of 270.30 mg/g. In addition, adsorption kinetics evaluations showed that adsorption equilibrium occurred in 5 h, with about 75 percent of the optimum adsorption capacity achieved in the first hour.

#### 2.1.5. Biomaterials

Because of their affordability and environmental friendliness, a variety of natural and engineered biomaterials, like waste from tea [44], algae [45], leaves [46], husks, and more, are being used to remove fluoride from water. Kazi et al. [47] used *Cucumis pubescens* in the presence of a ions in water to conduct defluoridation studies. Surprisingly, the presence of  $\text{Na}^+$  had no obvious effect on the biosorbent's ability to remove fluoride. This study also considered electrolytes such as  $\text{K}^+$ ,  $\text{Ca}^{2+}$ ,  $\text{Mg}^{2+}$ ,  $\text{Fe}^{3+}$ ,  $\text{Se}^{4+}$ ,  $\text{Cl}^-$ ,  $\text{SO}_4^{2-}$ ,  $\text{Br}^-$ , and  $\text{NO}_3^-$ .

Grafted jute was chosen by Manna et al. [48] as a potential adsorbent for defluoridation. The fluoride adsorption of grafted jute powder was substantially greater than that of untreated jute powder. Infrared spectroscopy and X-ray photoelectron spectroscopy indicated that hydrogen bonds, protons, and carbon-fluoride bonds were responsible for the fluoride deposits on grafted jute. Also, as a potential adsorbent for defluoridation, Xu et al. [49] produced porous starch (PS) filled with typical metal ions (Zr, Al, Fe, and La). Based on the results, PS-Zr had a better ability to remove fluoride. Sankararamkrishnan et al. [50] created Zerovalent-iron (ZVI)/Zirconium (IV) (Zr)/ZVI-Zr-doped cellulose nanofibers by extracting cellulose nanofibers from bagasse. Among these materials, ZrZVICNF demonstrated a significantly greater Langmuir adsorption capacity, reaching 35.70 mg/g, compared to several commercial adsorbents.

#### Industrial By-Products for Fluoride Removal

Various industrial residues were utilized effectively for the adsorptive removal of contaminants from water, notably fluoride, resulting in excellent defluoridation performance. A study of the elimination of fluoride capacities of flue gas desulfurization gypsum (FGD) was carried out by Kang et al. [51]. By using FGD, they were able to significantly reduce fluoride, achieving a 93.31% decrease and bringing the concentration down from 109 to 7.3 mg/L. At 1 g/L FGD, kinetic analysis showed a theoretical fluoride capacity of 96.90 mg/g. Zhou et al. [18] reported an inventive method of producing a bimetallic adsorbent through the activation of zirconium-immobilized alkali-active chrome-tanned leather particles (ZACLIP). The Langmuir equation accurately described the fluoride adsorption onto ZACLIP, indicating a remarkable 30.49 mg/g fluoride removal capability.

#### 2.1.6. Polymers and Resins

Adsorbents classified as polymers and resins are key types of materials utilized to remove cationic and anionic pollutants in wastewater as well as water. Their irregular, macromolecular, three-dimensional structure within the hydrocarbon chain system essentially makes them suitable as resources for fluoride removal.

##### Polymers

The surface properties of polymers can be altered to enhance their effectiveness in binding with fluoride. In recent years, polymers have attracted the attention of researchers more and more because of their high surface activity, adaptable surface properties, affordability, and suitability for the creation of adsorbents. As an outcome, there has been a lot of interest in utilizing polymers to remove fluoride from aqueous solutions. Fe-Al-Ni tri-metal oxides were deposited on two different biopolymers, pectin and alginic, by Raghav and Kumar [52]. The greatest adsorption capacities for Fe-Al-Ni/pectin and Fe-Al-Ni/alginate were found to be 285 mg/g and 200 mg/g based on the Langmuir isotherm, emphasizing pectin's better adsorption capacity. Extensive research on fluoride absorption was carried out by Wang et al. [53], applying Carboxymethyl Cellulose (CMC) microspheres associated with lanthanum (III). The findings showed that, in contrast with CMC-La, linked CMC-La had superior acid and alkali tolerance as well as a higher decomposition temperature

(200 °C vs. 190 °C). The highest removal efficiencies of CMC-La and linked CMC-La were around 98.85% and 99.31% at pH 4.0. Chen et al. [54] looked at fluoride removal with the PPy/TiO<sub>2</sub> composite. The findings of the characterization showed that the composites had a sufficient specific surface area and a large number of positively charged nitrogen atoms. By fitting the experimental findings to the Langmuir isotherm, the maximum fluoride adsorption capacity of 33.18 mg/g was found. Sharma et al. [55] employed iron metal to modify poly(amidoxime). Despite its modest adsorption capacity (3.20 mg/g), the pectin-g-poly(amidoxime)-Fe complex was found to exhibit selectivity for fluoride ions, as indicated in the study.

### Resins

Resins are often used as fluoride removal adsorbents due to their high adsorption capacity, versatility to a range of operational circumstances, and excellent durability. To act as a base anion exchange resin, Rungrodnimitchai and Kotatha [56] synthesized chemically altered ground tire rubber. Comparing this modified ground tire rubber to commercial resin, the modified rubber showed a greater rate constant for fluoride elimination. The modified ground tire rubber's maximal defluoridation capability was found to be 0.86 mg/g when heated in a microwave and 0.83 mg/g when heated using a traditional heating method. Research was conducted by Phillips et al. [57] to determine how well Haix-Fe-Zr and Haix-Zr resin beads removed fluoride. The outcomes showed that when it came to eliminating fluoride from contaminated waters, Haix-Fe-Zr resin beads performed more efficiently than Haix-Zr resin beads. The fluoride removal process involved shaking with Haix-Fe-Zr resin beads for a duration of fifteen minutes.

#### 2.1.7. MOFs for Fluoride Removal

A coordination network comprising organic ligands featuring potential gaps is referred to as a metal–organic framework, abbreviated as MOF [58]. The interaction between chemical ligands and the apparent arrangement of metal ions or clusters within MOFs enables the creation of diverse framework pore shapes and the manifestation of exceptional adsorption characteristics [59]. MOF materials are characterized by three key attributes: a substantial specific surface area, a porous structure, and structural and functional versatility. Additionally, they possess unsaturated metal sites. MOFs have been used by several researchers in the past few years to efficiently remove excessive fluoride ions from water in an effort to lower fluoride levels to a safe level. Therefore, a key factor in the elimination of fluoride process is the pH of the solution, which affects the surface charge of the adsorbents.

#### Fumarate-Based MOFs

By using a hydrothermal technique, Karmakar et al. [60] produced aluminum fumarate (AlFu) MOFs. It was found that these AlFu MOFs have microporous features, with a tremendous surface area of 1156 m<sup>2</sup>/g and an average pore size of 17. The adsorption capacity was maintained consistently at almost 100% throughout pH values of 2 and 7, with a little decrease noted at pH 8. At every temperature, the Freundlich isotherm approach suited the experimental findings more effectively than the Langmuir model. Since the Freundlich isotherm illuminated fluoride adsorption on heterogeneous surface sites. It supports multilayer adsorption and works well for adsorbents like zeolite and metaettringite. In addition, at 293 K, the AlFu MOFs exhibited a phenomenal maximum adsorption capacity of 600 mg/g.

In order to eliminate fluoride from brick tea infusion, Ke's group utilized two fumarate-based MOFs, MOF-801 and CaFu [61]. The fluoride adsorption capacities were determined to be 38.60 mg/g and 45.72 mg/g at temperatures of 308 and 318 K. Adsorption in this particular case of MOF-801 increased at lower pH values and dropped down significantly at pH 5. Moreover, nontoxic homologous calcium fumarate (CaFu) MOFs were developed and utilized to remove fluoride from the infusion of brick tea. A total of 166.11 mg/g of

fluoride was found to be the maximal absorption capacity at 373 K while the isotherm data were properly fitted to the Langmuir model.

#### Other MOFs

To mitigate fluoride levels in water, Zhao et al. [62] devised a novel metal–organic framework, Ce-1,1'-biphenyl-4,4'-dicarboxylic acid (Ce-bpdc). Utilizing the Langmuir model, they determined that this framework exhibited a remarkable maximal adsorption capacity of up to 45.50 mg/g at 298 K, accompanied by an impressive removal efficiency exceeding 80%. Wang et al. [27] investigated MIL-96(Al)'s defluoridation potential using a granular structure based on rice. The results showed that MIL-96(Al) outperforms activated alumina, which is often utilized, with a predicted fluoride adsorption capacity of 42.19 mg/g at 298 K. The adsorption isotherm was well represented by the Langmuir model. Furthermore, Ma et al. [63] used H<sub>4</sub>L1 and H<sub>4</sub>L2 as second guests to examine the fluoride adsorption characteristics of two novel lanthanide-based metal–organic frameworks, [Ce(L1)<sub>0.5</sub>(NO<sub>3</sub>)(H<sub>2</sub>O)<sub>2</sub>]<sub>2</sub>DM (1) and [Eu<sub>3</sub>(L2)<sub>2</sub>(OH)(DMF)<sub>0.22</sub>(H<sub>2</sub>O)<sub>5.78</sub>]. When they were evaluated at different periods of uptake, 1 was shown to have a much greater capacity for adsorbing fluoride ions (103.95 mg/g) and to absorb them more quickly (1.79 g mg<sup>-1</sup> min<sup>-1</sup>) than 2.

#### 2.1.8. LDHs for Fluoride Removal

LDHs, also known as layered double hydroxides, encompass hydrotalcite and similar compounds. The creation of hydrotalcite-like intercalation materials involves a supramolecular process achieved through the intercalation of these substances. LDHs consist of interlayer anions and positively charged main laminates, held together by non-covalent bonds. The structural properties of LDHs allow the interlayer anions to undergo exchange with a wide array of anions, encompassing inorganic, organic, homologous, heteropoly acid ions, and coordination compound anions. A recent breakthrough focused predominantly on the utilization of Mg–Al LDHs for fluoride removal. Huang et al. [64] successfully synthesized Mg–Al LDHs with Cl<sup>-</sup> and CO<sub>3</sub><sup>2-</sup> serving as interlayer anions using a surfactant-free solvothermal technique. These hierarchical Mg–Al LDHs revealed a notable fluoride removal capacity of 28.60 mg/g. Investigating the fluoride removal from starch-stabilized Mg–Al LDHs, Liu et al. [65] highlighted that incorporating a small amount of starch significantly enhances fluoride removal efficiency. Ghosal and Gupta [66] explored the adsorption behavior of calcined Ca–Al–(NO<sub>3</sub>) LDHs, employing the response surface methodology to assess the impact of temperature and other key process variables. The pH of the solution had minimal influence on adsorption. The anion order on adsorption capacity was PO<sub>4</sub><sup>3-</sup> > CO<sub>3</sub><sup>2-</sup> > SO<sub>4</sub><sup>2-</sup> > NO<sub>3</sub><sup>-</sup> > Cl<sup>-</sup>. Furthermore, the defluoridation potential of carbonate layered double hydroxides (LDHs) with varying cation compositions (M<sup>2+</sup> = Mg<sup>2+</sup>, Zn<sup>2+</sup>; M<sup>3+</sup> = Al<sup>3+</sup>, Fe<sup>3+</sup>) and M<sup>2+</sup>/M<sup>3+</sup> molar ratios were examined by Dore and Frau [67]. Among these compositions, the 3MgAlFe-cal phase, resulting from calcination with a Mg/(Al + Fe) ratio of 3/(0.5 + 0.5), exhibited the highest defluoridation capacity, capable of adsorbing up to 92.30 mg/g of fluoride.

### 3. Membrane Technology Process

Membrane processes, including electrodialysis, reverse osmosis, ion exchange, and nanofiltration, are an attractive substitute for conventional techniques for removing ions from aqueous solutions due to their high efficiency, selectivity, and possibility for ion fractionation. It is now possible to extract fluoride and other ions from water solutions using electrodialysis and ion-exchange membranes. When an applied electric potential difference is present, ions can travel via ion-exchange membranes using this very simple technique. As a result, there is increasing interest in using membrane technologies to generate drinking water on a small scale. To extract certain ions from raw water sources, new techniques including electrodialysis, ultrafiltration, nanofiltration, and reverse osmosis (RO) are being developed more often.

Membrane separation technologies, including microfiltration, ultrafiltration, nanofiltration, reverse osmosis, and electrodialysis, have gained industrial prominence, serving various sectors such as water purification, seawater desalination, and environmental remediation across diverse industries. These advanced membrane technologies offer several advantages over traditional methods and are widely employed as pretreatment in desalination and in treating fluoride-containing wastewater. The concept of size exclusion plays a critical role in membrane separation, where membranes can be efficiently separated from water using conventional membrane separation techniques. Additionally, Membrane Distillation (MD) has gained significant attention as a water treatment method, particularly for highly salinized solutions. While reverse osmosis (RO) membranes have demonstrated effective fluoride removal capabilities, they are hampered by membrane fouling and high energy consumption. Low-Pressure Membranes (LPMs), offering cost-effective solutions with filtration pressures a fraction of RO membranes, have gained global adoption. The synergy of adsorption and membrane separation presents an efficient fluoride removal approach while minimizing secondary contamination risks. Identifying materials that can serve as both adsorbents and membranes becomes pivotal. Among MD configurations, Direct Contact Membrane Distillation (DCMD) is the most generally used, although it often leads to substantial heat losses due to high feed temperatures. Vacuum-Enhanced DCMD (VEDCMD) has been introduced to generate a higher vapor driving pressure, even at lower input temperature ranges. Traditional separation techniques, namely skimming, sedimentation, air flotation, and centrifugation, while broadly utilized, often fall short in capturing emerging pollutants. Porous adsorbents, while versatile, may lack selectivity and generate secondary waste. Ion exchange resins are effective for heavy metal removal but are sensitive to operating conditions. Polymer membranes offer advantages such as reduced energy consumption, chemical-free operation, and continuity, with advancements leading to Mixed Matrix Membranes (MMM), Thin-Film Nanocomposite Membranes (TFN), nanofiber membranes, and zwitterionic membranes. Thin-Film Composite Membranes (TFC) have become prominent in water purification, though fouling can diminish their performance over time. Thin-Film Nanocomposite (TFN) membranes, boasting anti-fouling properties, have emerged as an alternative solution. Researchers have developed various types of TFNs for water purification. The discussion that follows delves into several membrane-based technology categories [68].

### 3.1. Nanofiltration Membrane

In recent years, polymer-based nanofiltration has played a pivotal role in applications like water purification, pharmaceuticals, and biotechnology. The increasing deterioration of the environment and population growth have heightened the importance of purifying seawater for drinking purposes, prompting a significant rise in the deployment of nanofiltration (NF) membranes for tertiary water treatment, particularly for ultrapure water production. NF, a relatively recent advancement in membrane technology, can operate in aqueous and non-aqueous settings, offering properties intermediate between ultrafiltration (UF) and reverse osmosis (RO). These membranes often carry negative surface charges due to membrane charges playing a crucial role in their function. NF technology is extensively utilized in various industrial applications for water and wastewater treatment (WWT), with a primary focus on the selective removal of ions and organics. It has received attention when coupled with UF and RO for improved separation performance and finds particular utility in seawater desalination applications. NF functions in a moderate pressure range of around 0.5 to 1.5 MPa and shows great promise for treating water. It efficiently removes essential minerals from drinking water while preserving small organic molecules and some inorganic salts. This state-of-the-art technology has the following features: stability, minimal chemical use, energy economy, a tiny carbon footprint, ease of maintenance and management, and the potential for zero emissions. Due to this, NF separation technique is considered the next generation of drinking purification methods and an efficient way to produce high-quality drinking water. Cellulosic materials offer

distinct advantages, including low cost and eco-friendliness, making them a promising choice for sustainable development. Leveraging biomass energy efficiently can lead to a more ecologically sustainable path, contrasting with the environmental issues associated with synthetic polymer products. This review examines the most recent developments in cellulose nanofiltration membranes and their applications, delivers an in-depth review of the fabrication approaches of composite nanofiltration membranes with a particular focus on pore size-management strategies, and provides recommendations and further investigations for the growth of improved cellulose-based NF membranes. In the context of water and energy, nanofiltration technology based on Thin-Film Composite Membranes (TFC) is instrumental for tailor-made ion separation, driven by its energy-efficient method and capability for selective ion separation through Donnan exclusion and size-sifting effects. Donnan exclusion is the selective separation of ions by a charged barrier, allowing ions of opposite charge to pass while repelling those with the same charge. The development of highly selective NF membranes is essential to meet the growing demands for efficient ion separation, particularly in water and energy-related fields. Notably, depending on membrane surface charge, pore size, and chemical affinity, the pressure-driven processes of NF and RO both retain certain ions, particles, or compounds. Although RO membranes have holes smaller than 1 nm and a molecular weight cutoff (MWCO) of fewer than 200 Da, they are also more efficient at eliminating tiny organic compounds and ions that are dissolved than NF, which usually has a MWCO of 200–1000 Da. These features have increased the requirement for NF and RO membranes in a variety of separation uses, particularly in the treatment of water and effluent. They have even been used to separate biological components like sugars and polyphenols from materials like apple juice, with rejection rates approaching 95% [69].

### 3.2. Microfiltration Membrane

Porous-structured ceramic microfiltration membranes were created using kaolin, feldspar, quartz, boric acid, activated carbon, sodium metasilicate, and titanium dioxide using the conventional paste casting technique. These membranes were shaped like round disks, measuring 5 mm in thickness and 40 mm in inner diameter. The membranes went through characterization employing techniques such as thermogravimetric analysis (TGA), particle size distribution (PSD), X-ray diffraction (XRD), and scanning electron microscopy (SEM) to evaluate the effect of the maximum sintering temperature on their structure, permeability, and mechanical characteristics. The produced membranes were first dried at 120 °C and 250 °C for 24 h each, and then they were sintered for 6 h at 850 °C, 900 °C, and 950 °C. Pore size distribution, porosity, and average pore size were found to be important structural factors. Only pure water permeability tests were used to evaluate the performance of the membrane. The average membrane pore size increased from 1.59 µm to 2.56 µm, and the membrane support porosity decreased from 18.88% to 5.59% when the sintering temperature was raised from 850 °C to 950 °C, according to the data. Additionally, the corrosion resistance of the membrane was tested using an acid and base, and the results showed no appreciable weight loss [69]. These ceramic membranes were estimated to have cost \$92/m<sup>2</sup>, which puts them in the affordable range for microfiltration in a variety of industrial applications, given the market pricing of the inorganic precursors.

Chemical alteration was applied to PVDF (0.45 µm, Millipore, Burlington, MA, USA, HVLP02500) microfiltration (MF) membranes [70] and includes the following: (1) The process involves first immersing virgin membranes in a KOH solution containing TBAF and then dipping them into an aqueous solution of NaHSO<sub>3</sub> that includes H<sub>2</sub>SO<sub>4</sub>; (2) a TMC hexane solution; and (3) immersion in a SiO<sub>2</sub> suspension (0.05, 0.1, and 0.5 wt%). The resultant SiO<sub>2</sub>-modified membranes were then (4) impregnated with CuCl<sub>2</sub> in a shaker and agitated into a K<sub>3</sub>[Fe(CN)<sub>6</sub>]•3H<sub>2</sub>O solution. The membranes were then carefully cleaned with ultrapure water and labeled as SiO<sub>2</sub>/PVDF-0.05%, SiO<sub>2</sub>/PVDF-0.1%, and SiO<sub>2</sub>/PVDF-0.5%, respectively. SiO<sub>2</sub>/PVDF membranes filled with CuFC were obtained by rigorous washing to eliminate residuals. The CuFC loading process was repeated one to three times

to facilitate crystal growth. The resulting CuFC/SiO<sub>2</sub>/PVDF membranes were rinsed with ultrapure water, dried, and stored in ultrapure water until use [71].

### 3.3. Ultrafiltration Membrane

Fluoride removal can be achieved through various methods, including ion-exchange, precipitation, adsorption, and membrane-based techniques. Among these, Micellar Enhanced Ultrafiltration (MEUF) stands out as a promising membrane-based approach. Ultrafiltration (UF) membranes, developed since their initial use in 1970 for electrophoretic oil separation, have evolved into a reliable, clean, cost-effective, and efficient tool for separating diverse components and contaminants from water and wastewater. UF has a rich history dating back to 1907 when Benchold first introduced the concept, describing it as a method to mechanically separate components from mixtures using membranes operated under pressure, making it highly attractive for groundwater and surface water treatment, especially for removing particles, colloids, and microorganisms [72]. Additionally, the pretreatment of UF with coagulants can enhance water quality and minimize membrane fouling. MEUF employs surfactants to form micelles retained by UF membranes [73].

MEUF was explored for fluoride removal in batch operations employing cetylpyridinium chloride (CPC), a cationic surfactant, and ultrafiltration membranes based on polyether sulfone (PES). Phase inversion was used to create the PES membranes, which showed ultra-porous characteristics with a molecular weight cut-off (MWCO) of 50 kDa. With response surface methodology (RSM) and central composite design (CCD) in a 20-run factorial design, fluoride removal with MEUF was optimized. Concurrently, a coagulation-ultrafiltration (UF) method was suggested for the treatment of fluoride wastewater. This method uses wastewater from chemical mechanical polishing (CMP) as a coagulant. The elimination of fluoride, turbidity, and membrane fouling resistance of different combinations of wastewater were assessed [69].

The MEUF process relies on conventional UF principles and employs surfactants with hydrophobic tails and hydrophilic heads [74]. Micelles formed by surfactants reduce surface tension and can encapsulate impurities through electrostatic interactions or within their hydrophobic cores. These micelles, with their distinct surface charges, can bind oppositely charged ions, and their larger size compared to membrane pores allows for their separation during ultrafiltration. UF has gained prominence in drinking water production due to its lower energy consumption relative to RO and NF, as well as reduced membrane costs. While UF is primarily used for macromolecular solution concentration, its application for ionic species separation or concentration in solution has been limited. Recently, UF has been explored for the recovery of PSA polyelectrolytes following forward osmosis (FO), demonstrating high rejection rates and minimal product water contamination.

The MEUF process offers several advantages, including low energy consumption, high removal efficiency, and impurity recovery potential. It is also less energy-intensive than traditional cleaning methods and can facilitate the recovery of valuable compounds. However, challenges such as contamination and concentration polarization must be addressed. Membrane fouling can occur due to factors like gel layer compression, impurity clogging, concentration polarization, and solid adsorption onto the membrane surface or within the membrane matrix. Concentration polarization, for example, can result in the deposition of micelles or impurities on the membrane surface, forming a fouling layer that reduces permeate flow. Additionally, small amounts of surfactant monomers and unbound pollutant molecules may permeate through the membrane.

### 3.4. Forward Osmosis

For many years, the world has struggled with freshwater shortage, which has led to 685 studies into desalination techniques that employ membrane-based technologies like reverse osmosis (RO) and forward osmosis (FO). Osmosis, which is defined as the spontaneous passage of a solvent across a semi-permeable membrane propelled by a concentrated solute gradient, is used in the development of new membrane technologies

such as pressure-delayed osmosis and forward osmosis [75]. These technologies, which mark a new chapter in membrane development, rely on thin-film membranes supported by porous layers and scalable membrane materials. Performance is greatly influenced by important membrane properties such as pore structure, hydrophilicity, surface roughness, and water flow. Forward osmosis (FO), one of the latest desalination techniques, leverages the osmotic pressure gradient across a semipermeable membrane to produce freshwater from various water sources. The effectiveness of FO processes hinges largely on the performance, recyclability, and cost of the draw solution (DS) used in conjunction with the FO membrane. The DS plays a vital role in extracting water molecules from wastewater or seawater, making it a critical component in any FO process. Ideally, an optimal draw solution should possess a straightforward regeneration mechanism, low reverse flux, and high osmotic pressure.

FO uses semi-permeable membranes, which allow water to pass through because of the differential in osmotic pressure between the draw and feed solutions. FO has gained substantial attention as an attractive membrane-based desalination technology owing to its potential cost-effectiveness, reversibility of fouling, and high rejection of various contaminants, aligning with environmental concerns [76]. The driving force behind water migration into the higher osmotic potential draw solution (DS) arises from the osmotic gradient established between two streams with differing salinities and separated by a semi-permeable membrane. FO membranes typically fall into three categories: (1) thin-film composite (TFC) membranes, (2) self-assembling layer-by-layer membranes, and (3) selective thin films that function independently without support. TFCs, featuring a selective polyamide layer atop a microporous substrate, have been widely employed in FO applications [77].

FO occurs through the use of the natural osmotic mechanism, which involves moving water molecules from salinized feedwater across a semipermeable membrane and into a more concentrated draw solution (DS). The driving force is the naturally occurring osmotic pressure differential between the feed solution (FS) and the DS [74]. FO has a number of benefits over conventional hydraulic pressure-driven membrane processes, including a lesser risk of fouling and a lower energy need. Compared to pressure-driven alternatives, FO runs at low or no hydraulic pressures, has good contamination rejection, and has less membrane fouling. The apparatus required is simple, and supporting the membrane is not as difficult. FO is useful for food and pharmaceutical processing because it can concentrate the feed stream without needing high temperatures or pressures that might damage the feed solution [76].

FO also holds potential for precise and gradual drug release in medical applications, particularly for drugs with limited oral bioavailability due to poor solubility or permeability. However, FO faces challenges, such as solute evolution/regeneration, the need for robust FO membranes for industrial-scale use, and the possibility of unintended DS incorporation into final products. The selection of appropriate solutes is crucial for achieving energy-efficient FO processes. Energy consumption primarily arises from DS separation or regeneration, and finding recyclable and cost-effective solutes is essential. Moreover, further research is needed to address issues like fouling and concentration polarization (CP) [78].

### 3.5. Reverse Osmosis

Reverse osmosis (RO) is widely acknowledged for its dense, non-porous membrane structure, while UF and MF are known for their porous membranes. Successful fluoride removal from water using NF/RO has been documented. RO stands as a well-established and readily available technology in the water treatment sector. It operates under pressure control, employing semi-permeable membranes to eliminate dissolved contaminants in the feed water through a combination of charge exclusion, size exclusion, and physicochemical interactions among solvents, solutes, and membranes [79].

The fundamental mechanism governing liquid transport across RO membranes is “solution diffusion”, where there are no open channels for pore flow. As an overpressure



compels liquid through the membrane in the opposite direction to natural osmosis, it creates a lateral chemical concentration gradient across the membrane [73]. In the context of contaminated water, water molecules migrate from areas of high concentration to areas of low concentration, displacing and accumulating contaminants on the influent membrane's surface. RO proves to be a viable choice for recovering diluted draw solutions due to its high-water recovery rate and effective salt removal capacity.

To safeguard the RO membrane from fouling and debris, the FO membrane can remove a broad range of impurities, and the draw fluid directed to the RO unit becomes diluted after undergoing the FO process in its initial stage. Consequently, significant cost savings can be anticipated with RO desalination. Recent research indicates that utilizing a hybrid FO/RO process for desalinating brackish water and wastewater is both technically and economically feasible, with energy savings potentially stemming from the cost-effectiveness of pretreatment and RO processes [78].

The primary mechanisms responsible for perfluoroalkyl acid substance (PFA) repulsion by NF and RO membranes encompass steric (size) exclusion, solution diffusion, and electrostatic interactions. Generally, RO membranes possess a denser structure than NF membranes, resulting in a higher steric exclusion capacity for RO, which accounts for its superior removal of organics. RO flux correlates with the net driving pressure, akin to NF. Water flux closely correlates with transmembrane pressure, while solute transport remains unaffected by applied pressure. Therefore, raising the pressure augments water flux without altering solute permeability, thereby increasing the removal rate and salt removal rate at high pressures.

When smaller solutes of PFAs were introduced into the PFHxA removal investigation, commercial RO membranes rejected them because the water dissolved and spread across the membrane, trapping the compounds. Water is not the only substance that can compete with other substances for absorption into the polymer and diffusion across the polymer-free region, even though solution diffusion is the predominant method of separation. As a result, it has not been noted that PFAs in the permeate may cross RO membranes. The influence of concentration polarization (CP) cannot be disregarded in RO processes, especially when the solute flow rate is low. A low flow rate characterized by a low Reynolds number significantly elevates solute concentration and osmotic pressure at the membrane surface, leading to heightened CP. This phenomenon simultaneously reduces and excludes water flow. For instance, CP at the liquid interface has been previously considered in calculating the removal rate during PFHxA treatment [69].

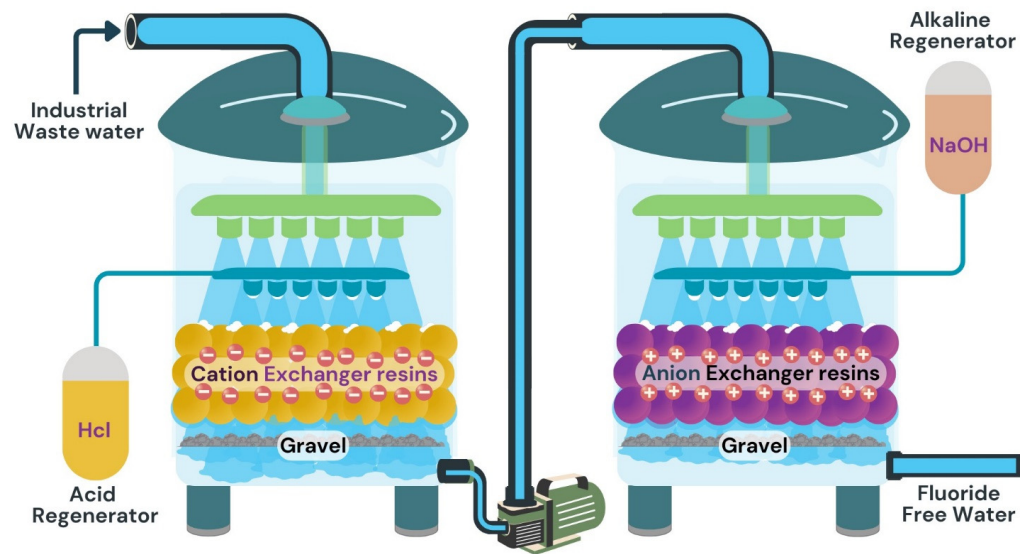
#### 4. Ion Exchange Process

Fluoride can also be removed by ion exchange; however, the method's efficiency is significantly low, which is hindered by the existence of other anions, including nitrates, sulfates, phosphates, carbonates, etc. While utilizing anion-exchange resins, cation/chelating-type resins should be considered for the ion-exchange/sorption approach of fluoride removal shown in Figure 3.

Ion exchange encompasses a class of chemical reactions that has found widespread application in various industries, particularly in the beverage sector [80]. In the context of water treatment and the selective removal of pollutants, ion exchange processes utilizing ion exchange membranes like electrodialysis, diffusion, and Donnan dialysis are separation processes where ions are transported across a charged membrane, driven by the concentration gradient of counter-ions. Electrode ionization and capacitive deionization have emerged. These processes facilitate the removal of small molecular ions from nutrient solutions by leveraging electrochemical gradients [79].

The main components of electrical membrane processes are ion-exchange membranes, resembling plate-like ion-exchange resins. One prominent instance consists of ion intercalation and subsequent redox reactions that are seen in electrodes made of Prussian Blue (PB) and its analogs (PBAs) [70]. Two forms of ion exchange membranes may be distinguished from these: (1) cation exchange membranes, which have negatively charged groups affixed

to a polymer matrix, and (2) anion exchange membranes, which have positively charged groups embedded in a polymer matrix [81].



**Figure 3.** Ion exchange fluoride removal.

Selective exchange with mobile cations is made possible by cation exchange membranes, which hold fixed negative charges in electrical equilibrium within the polymers. Zirconium-impregnated hybrid anion exchange resin (HAIX-Zr) is used in practice to remediate groundwater polluted with fluoride.  $ZrO_2$  nanoparticles are impregnated onto a polymeric anion exchange resin to generate HAIX-Zr resin, which has fast fluoride absorption—60% elimination in 30 min. The Freundlich adsorption isotherm model is the most accurate representation of the apparent second-order kinetic model that describes the kinetics of fluoride adsorption. The efficacy of HAIX-Zr in removing fluoride from groundwater is demonstrated by the determination of the maximal fluoride absorption capacity, which is 12.0 mg/g [82,83].

Strong Base Ion Exchange (SBIX) stands out as a highly effective technology for removing several regulated oxyanions from drinking water. Some exchange resins can be regenerated using a concentrated salt solution to yield brine. The ion storage capacity, critical for desalination through cation intercalation, hinges on the cathode's particle storage limit and is directly proportional to the charge storage capacity, measured in mAh/g, provided the electrode selectively adsorbs cations or anions [83].

In ion exchange, solid materials with specific charges are employed to separate liquid phases. Ion exchange membranes, akin to sheet-shaped ion exchange resins, exhibit distinct differences in mechanical properties and spreading behavior when compared to exchange resins. Ion exchange resins are mechanically fragile and tend to swell considerably in dilute electrolyte solutions. To address this issue, a film is typically created on a stable reinforcing material to impart the necessary strength and dimensional stability. Presently, two technologies are employed in ion exchange membrane production, resulting in either a more heterogeneous or homogeneous structure.

Ion exchange membrane processes, where ion exchange membranes serve as a pivotal component, can be categorized into three types: (1) electrode ionization processes, (2) electrosynthesis processes, and (3) electromembrane energy conversion processes. The first type employs an electric potential gradient to eliminate charged components from a solution, such as dispersed salts. The second type combines ion transport with electrochemical reactions to produce specific chemicals, like bases and chlorine, from corresponding salts. The third type entails converting chemicals into electrical energy, as seen in fuel cells [81].

While ion exchange membranes find applications in various domains, including electrochemical synthesis and energy conversion, this discussion primarily focuses on their

role in water treatment. It is essential to address challenges, such as salt ion contamination when strong acids and bases are involved, as well as the inefficiencies in removing heavy metals using ion exchange resins under non-ideal conditions. Freshwater shortage is a problem that impacts a large number of people worldwide; 2.7 billion people experience it for at least one month out of the year, and another 2.4 billion are at risk of contracting water-borne illnesses. Every year, this tragedy takes the lives of approximately two million people, mostly children. Furthermore, the outflow of H and OH ions across monopolar anion and cation exchange membranes affects continuous consumption, especially when high acid and base concentrations are required. This results in significant salt contamination and low energy efficiency.

## 5. Electrodialysis

In addition to adsorption, membrane separation methods like ultrafiltration (UF), nanofiltration (NF), reverse osmosis (RO), and electrodialysis (ED) have been advocated as preferred techniques for various applications. Among these, the ED process stands out as an intriguing method for selectively removing specific contaminants, such as excessive fluoride ions, from drinking water. However, one persistent challenge with NF and RO membranes is their elevated energy consumption owing to high-pressure operation.

Reverse osmosis, ultrafiltration, nanofiltration, and electrodialysis have all garnered attention as superior approaches for selectively extracting specific ions from raw water, surpassing traditional adsorption methods. Within this spectrum of options, the ED process has emerged as a captivating technique for efficiently eliminating targeted contaminants, particularly the excess fluoride ions present in drinking water. The ED process employs direct current (DC) as the driving force for ion transfer, facilitated by ion exchange membranes. This process is utilized for the dilution or desalination of electrolyte solutions, thereby concentrating the desired substances. The present study entails a comprehensive investigation of the ED process's efficacy in removing fluoride ions from groundwater sources. Previous research efforts have explored the ED process using a constant voltage setup.

According to Faraday's law, the extent of desalination achieved in the ED process is directly proportional to the electrical current passed through the system. To comprehensively analyze the desalination phenomenon, including its interaction with coexisting ions, the constant current system is considered the most suitable approach.

Different types of contaminant removal take place in the ED process. A few examples are  $\text{ClO}_4^-$  (perchlorate),  $\text{Zn}^{2+}$  (zinc),  $\text{F}^-$  (fluoride),  $\text{NO}_3^-$  (nitrate),  $\text{Br}^-$  (bromide),  $\text{Na}^+$  (sodium),  $\text{Sr}^{2+}$  (strontium). By using the electrodialysis process, the percentage the fluoride removal ranges between 95 and 96%. Some of the parameters that affect this treatment are temperature (T), the pH of the feeding solution, electric current (I), and electric power (P). The ion exchange membrane method of electrodialysis, which removes ionic components from aqueous solutions by pushing the process forward with an electrical field (the driving force of the ED process), was selected for this investigation. Research has been conducted on the electrodialysis method used to extract nitrate and fluoride ions from simulated (photovoltaic) PV industry wastewater, as well as the competition between these two ions during that process. Using artificial solutions that mimicked PV cells rinsing waste fluids, the main operational factors influencing electrodialysis performance, such as current intensity, initial pollutant concentrations, and pH, were investigated. A heating system was not employed since it was believed that a temperature difference of less than 2 °C would have no major effect on the results. Instead, NaF and/or  $\text{NaNO}_3$  were dissolved in deionized water at different concentrations to create the synthetic solutions used in the batch testing. In the case of fluoride removal, NaF solutions were introduced to the diluted compartment at values ranging from 120 to 180 ppm. A second, less concentrated NaF solution was introduced to the concentrate compartment.  $\text{NaNO}_3$  solutions were introduced into the diluted compartment at different concentrations ranging from 750 to 2000 ppm in the nitrate removal condition [82].

An electro dialytic installation called the PCCCEL BED-1-System was used to conduct the study (PCCCell GmbH, Heusweiler, Germany). There was a 2 L tank for the dilute and concentrate (each) and a 9 L electrode solution tank. The electrode rinsing bath consisted of a 0.05 mol/L sodium chloride solution. With a different rotameter and pump, each solution circulated in its own independent loop. According to the producer, each circulation loop can sustain a volume flow rate of between 10 and 100 L/h. The linear liquid velocity in the ED tests was measured to be 6.25 cm/s, while a flow rate of 90 L/h was established. A maximum output voltage of 24 V and an amperage of 5 A were the defining characteristics of the DC power supply. The electro dialytic stack was outfitted with ten anion exchanges, and the membrane stack contained 11 cation-exchange membranes. A total of ten pairs of electrolytic cells. Each electro dialytic cell had a thickness of 0.5 mm, and the membranes were spaced from the electrodes by a distance of 0.025 mm. Each membrane's effective surface area was 64 cm<sup>2</sup>. The used membranes for ion exchange were of a unique design. Monovalent selective ion-exchange membranes are a subtype of these. The sample was taken from the fertilizer industry's wastewater effluent at a phosphate unit plant, which also makes aluminum fluoride. On the basis of ion transfer from the central compartment to the anodic compartment, it was examined how well electro dialysis reduced fluoride ion concentration and recovered phosphate ions. Equation (1) allows for the following calculation of membrane anion exchange, which facilitates the movement or transfer of phosphate and fluoride ions:

$$\text{Transfer of Ions (\%)} = (C_0 - C_t)/C_0 \times 100 \quad (1)$$

In this context, where the initial ion concentration in the input water is denoted as  $C_0$  and is measured in mg/L, while the current concentration is represented as  $C_t$  (mg/L), the electro-dialysis performance did not exhibit significant sensitivity to the applied current (ranging from 0.5 to 1 A) or the membrane surface area (varied between 100 and 200 cm<sup>2</sup>).

For instance, increasing the membrane surface area from 100 to 200 cm<sup>2</sup> resulted in a marginal increase in fluoride transfer, from 2.2% to 2.3%, with a current application of 0.5 A. The applied currents of 0.75 A and 1 A displayed similar trends, with fluoride transfer rates ranging from 2.2% to 2.3% and 2.7% to 4.6%, respectively, even considering the potential outlier. Phosphate ions exhibited minimal permeability, allowing only a small amount (less than 1% or 4.5 mg/L) of ions to pass through the membrane, suggesting that the middle compartment effectively facilitated phosphate recovery.

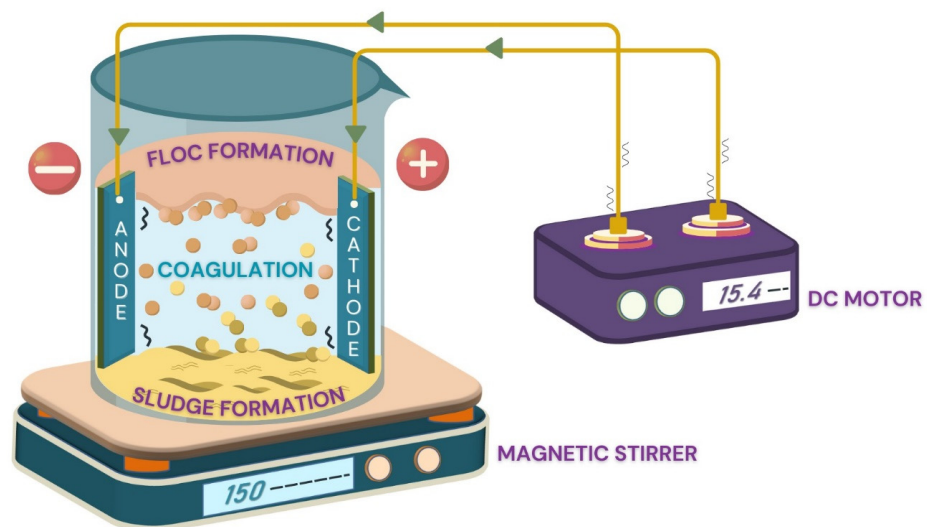
By removing an average of 2–3% of fluoride ions, it became possible to recover more than 99% of phosphate from the fertilizer effluent. These two major ion species appeared to compete through the membrane. Despite the removal of only 2–3% of fluoride ions, this recent study projected a mass transfer of up to 985 mg of fluoride, surpassing the results of earlier research by Othman et al. [82], which reported a maximum removal of 95% of initial fluoride ions. The outcomes align with the role of diffusion in explaining how monovalent ions exhibit higher transfer rates compared to divalent ions based on their ionic characteristics. Ion passage through the membrane appears to be highly competitive, with monovalent ions remaining unaffected by the arrangement of fixed ions within the membrane and moving freely. Additionally, their smaller radius allows monovalent ions to pass through the membrane's pore walls with minimal resistance compared to bivalent ions.

However, the transfer number was predominantly influenced by Gibbs hydration energy rather than Stokes radius, particularly for anions with the same ionic valence. Gibbs free energy ( $\Delta G$ ) indicates the energy driving fluoride ion migration in electro dialysis, with negative  $\Delta G$  signaling a spontaneous process. The Stokes radius reflects the hydrated ion size, influencing fluoride mobility through ion-exchange membranes. Furthermore, Banasiak and Schäfer's findings support the notion that ionic properties, including mobility and conductivity, significantly impact ion diffusion across membranes. The study by Kotare and Kultys also highlighted the limited permeability of anion-exchange membranes. It is worth noting that the fertilizer wastewater utilized in this

study had an extremely low pH, necessitating the use of a substantial quantity of a basic solution to elevate it to pH 6 in order to enhance fluoride ion removal.

## 6. Electrocoagulation

Due to its ability to reduce sludge production and eliminate the need for chemical additions, electrocoagulation (EC) is regarded as a successful approach for fluoride elimination from water. Mena et al. [83] successfully used the EC technique to eliminate fluoride from naturally occurring subsurface volcanic water. The original fluoride concentration, which was 6–9 mg F/L, was decreased to less than 1.5 mg F/L in treated water at ideal process conditions. Nevertheless, it was seen that the product water became more alkaline and that there was a build-up of scale on the electrode surface as illustrated in Figure 4. These undesirable events may lead to a decline in process effectiveness and an increase in energy demand.



**Figure 4.** Removal of fluoride through coagulation.

Electrochemical methods have demonstrated their effectiveness in removing fluoride ions from water [84]. These methods can be categorized as electrocoagulation, electrochemical reduction, electrochemical oxidation, indirect electro-oxidation, and photo-assisted electrochemical techniques [85]. Among these, electrocoagulation has found widespread application in wastewater treatment, addressing a variety of pollutants, including organic dyes, heavy metals, and hardness [86]. However, the practical utility of electrocoagulation has been hindered by the lack of a systematic approach to reactor design, operational procedures, and concerns regarding electrode reliability, particularly in the context of safe drinking water treatment.

To address these limitations, researchers have been motivated to develop operational-level electrocoagulation treatment systems as alternatives to dominant technologies like reverse osmosis, electrodialysis, and adsorption methods. Nonetheless, progress in this field has been impeded by the limited availability of suitable electrode materials [87].

Electrocoagulation systems offer the advantage of not requiring external coagulants since they generate coagulants by dissolving metal anodes. Aluminum electrodes have shown promise compared to iron electrodes for several reasons. Iron electrodes corrode uncontrollably in water, leading to the unregulated generation of iron-based coagulants, whereas aluminum electrodes form a surface passivating layer of aluminum oxide. Moreover, under controlled current flux, the release of aluminum ions ( $\text{Al}^{3+}$ ) can be regulated. Unlike ferric ions ( $\text{Fe}^{3+}$ ), aluminum ions tend to polymerize, forming  $\text{Al}(\text{OH})_{15}$  and  $\text{Al}_7(\text{OH})_{17}$  species, thereby limiting the presence of free  $\text{Al}^{3+}$  ions. This controlled generation of aluminum-derived coagulants allows for effective demand control, substantially reducing the need for alum addition and minimizing sludge production [88,89].

Consequently, sacrificial aluminum anodes in the electrocoagulation process are employed to simultaneously investigate the removal of hardness and fluoride from water. The removal of water hardness occurs through the precipitation of divalent ions on the cathode and the adsorption onto  $\text{Al}(\text{OH})_3$  flocs produced within the electrocoagulation cell, particularly in near-neutral pH conditions.

Optimized electrocoagulation cells exhibit enhanced removal of hardness (e.g.,  $\text{Ca}^{2+}$  and  $\text{Mg}^{2+}$ ) and fluoride from groundwater. The efficiency of ion removal from groundwater is influenced by water quality parameters such as pH, temperature, and ionic strength, as well as the operational parameters of the electrocoagulation cell. Achieving optimal electrocoagulation cell parameters necessitates a comprehensive analysis of major solutes like hardness in the water. Once optimization is achieved, the treated water composition must be assessed for trace constituents like fluoride. The electrode materials used in the electrocoagulation process significantly impact its performance. The electrodisolution of the anode releases coagulating agents that are essential for pollutant removal, with aluminum and iron being commonly used as anodes in studies on fluoride removal from groundwater and industrial effluents due to their favorable hydrolysis characteristics [90–92].

The use of NaCl as a supporting electrolyte to adjust conductivity to approximately 1200  $\mu\text{S}/\text{cm}$ , as suggested by M. López-Guzmán, is essential for efficient fluoride removal. Additionally, pH plays a crucial role in the fluoride removal process. Under alkaline conditions, the buffer capacity of the electrocoagulation process helps stabilize the pH of the solution. Low current densities maintain a constant pH rate in the solutions, while higher current densities may induce pH fluctuations due to increased hydrogen generation [93–95].

## 7. Conclusions

The challenge of water demand, exacerbated by pollution and climate change-induced water scarcity, is a monumental challenge in the twenty-first century. Excessive fluoride in drinking water, originating from various sources, presents a significant global health issue. The coexistence of pollutants can lead to complex, uncertain health effects, including cancer. Adhering to the World Health Organization's fluoride standards is crucial. However, many developing countries lack affordable water purification technologies, necessitating improved methods. Among the diverse range of fluoride removal techniques, adsorption, utilizing materials like activated carbon or specialized resins, stands out as a highly efficient, cost-effective, and environmentally friendly solution. Its practicality and adaptability make it the preferred choice for addressing the critical need for safe drinking water in various settings. Future perspectives include the continued development of adsorption technologies, increased accessibility to these methods, and a broader emphasis on sustainable and eco-friendly approaches to mitigate water quality challenges in an ever-changing world.

**Funding:** The research received no external funding.

**Conflicts of Interest:** The authors declare no conflict of interest.

## References

1. Schewe, J.; Heinke, J.; Gerten, D.; Haddeland, I.; Arnell, N.W.; Clark, D.B.; Dankers, R.; Eisner, S.; Fekete, B.M.; Colón-González, F.J.; et al. Multimodel assessment of water scarcity under climate change. *Proc. Natl. Acad. Sci. USA* **2014**, *111*, 3245–3250. [[CrossRef](#)] [[PubMed](#)]
2. Balaram, V.; Cobia, L.; Kumar, U.S.; Miller, J.; Chidambaram, S. Pollution of water resources and application of ICP-MS techniques for monitoring and management—A comprehensive review. *Geosystems Geoenviron.* **2023**, *2*, 100210. [[CrossRef](#)]
3. Ahmad, S.; Singh, R.; Arfin, T.; Neeti, K. Fluoride contamination, consequences and removal techniques in water: A review. *Environ. Sci. Adv.* **2022**, *1*, 620–661. [[CrossRef](#)]
4. Vences-Alvarez, E.; Velazquez-Jimenez, L.H.; Chazaro-Ruiz, L.F.; Diaz-Flores, P.E.; Rangel-Mendez, J.R. Fluoride removal in water by a hybrid adsorbent lanthanum–carbon. *J. Colloid Interface Sci.* **2015**, *455*, 194–202. [[CrossRef](#)] [[PubMed](#)]
5. Balarak, D.; Mahdavi, Y.; Bazrafshan, E.; Mahvi, A.H.; Esfandyari, Y. Adsorption of fluoride from aqueous solutions by carbon nanotubes: Determination of equilibrium, kinetic, and thermodynamic parameters. *Fluoride* **2016**, *49*, 71.
6. Ruan, Z.; Tian, Y.; Ruan, J.; Cui, G.; Iqbal, K.; Iqbal, A.; Ye, H.; Yang, Z.; Yan, S. Synthesis of hydroxyapatite/multi-walled carbon nanotubes for the removal of fluoride ions from solution. *Appl. Surf. Sci.* **2017**, *412*, 578–590. [[CrossRef](#)]

7. Kuang, L.; Liu, Y.; Fu, D.; Zhao, Y. FeOOH-graphene oxide nanocomposites for fluoride removal from water: Acetate mediated nano FeOOH growth and adsorption mechanism. *J. Colloid Interface Sci.* **2017**, *490*, 259–269. [[CrossRef](#)]
8. Zhang, J.; Chen, N.; Su, P.; Li, M.; Feng, C. Fluoride removal from aqueous solution by zirconium-chitosan/graphene oxide membrane. *React. Funct. Polym.* **2017**, *114*, 127–135. [[CrossRef](#)]
9. Zhang, J.; Chen, N.; Tang, Z.; Yu, Y.; Hu, Q.; Feng, C. A study of the mechanism of fluoride adsorption from aqueous solutions onto Fe-impregnated chitosan. *Phys. Chem. Chem. Phys.* **2015**, *17*, 12041–12050. [[CrossRef](#)]
10. Liu, Q.; Zhang, L.; Yang, B.; Huang, R. Removal of fluoride from aqueous solution using Zr (IV) immobilized cross-linked chitosan. *Int. J. Biol. Macromol.* **2015**, *77*, 15–23. [[CrossRef](#)]
11. Cho, D.W.; Jeon, B.H.; Jeong, Y.; Nam, I.H.; Choi, U.K.; Kumar, R.; Song, H. Synthesis of hydrous zirconium oxide-impregnated chitosan beads and their application for removal of fluoride and lead. *Appl. Surf. Sci.* **2016**, *372*, 13–19. [[CrossRef](#)]
12. Prabhu, S.M.; Elanchezhian, S.S.; Lee, G.; Meenakshi, S. Defluoridation of water by Tea-bag model using La<sup>3+</sup> modified synthetic resin@chitosan biocomposite. *Int. J. Biol. Macromol.* **2016**, *91*, 1002–1009. [[CrossRef](#)] [[PubMed](#)]
13. Liang, P.; An, R.; Li, R.; Wang, D. Comparison of La<sup>3+</sup> and mixed rare earths-loaded magnetic chitosan beads for fluoride adsorption. *Int. J. Biol. Macromol.* **2018**, *111*, 255–263. [[CrossRef](#)] [[PubMed](#)]
14. Li, C.; Chen, N.; Zhao, Y.; Li, R.; Feng, C. Polypyrrole-grafted peanut shell biological carbon as a potential sorbent for fluoride removal: Sorption capability and mechanism. *Chemosphere* **2016**, *163*, 81–89. [[CrossRef](#)] [[PubMed](#)]
15. Mudzielwana, R.; Gitari, M.W.; Akinyemi, S.A.; Msagati, T.A.M. Synthesis and physicochemical characterization of MnO<sub>2</sub> coated Na-bentonite for groundwater defluoridation: Adsorption modelling and mechanistic aspect. *Appl. Surf. Sci.* **2017**, *422*, 745–753. [[CrossRef](#)]
16. Wang, F.; Wang, K.; Muhammad, Y.; Wei, Y.; Shao, L.; Wang, X. Preparation of CeO<sub>2</sub>@SiO<sub>2</sub> microspheres by a non-sintering strategy for highly selective and continuous adsorption of fluoride ions from wastewater. *ACS Sustain. Chem. Eng.* **2019**, *7*, 14716–14726. [[CrossRef](#)]
17. Tian, Z.; Gan, Y. In situ synthesis of structural hierarchy flowerlike zeolite and its application for fluoride removal in aqueous solution. *J. Nanomater.* **2019**, *2019*, 2932973. [[CrossRef](#)]
18. Zhou, J.; Yu, J.; Liao, H.; Zhang, Y.D.; Luo, X.G. Facile fabrication of bimetallic collagen fiber particles via immobilizing zirconium on chrome-tanned leather as adsorbent for fluoride removal from ground water near hot spring. *Sep. Sci. Technol.* **2020**, *55*, 658–671. [[CrossRef](#)]
19. Chiavola, A.; D'Amato, E.; Di Marcantonio, C. Comparison of adsorptive removal of fluoride from water by different adsorbents under laboratory and real conditions. *Water* **2022**, *14*, 1423. [[CrossRef](#)]
20. Iizuka, A.; Ho, H.J.; Yamasaki, A. Removal of fluoride ions from aqueous solution by metaettringite. *PLoS ONE* **2022**, *17*, e0265451. [[CrossRef](#)]
21. He, J.; Yang, Y.; Wu, Z.; Xie, C.; Zhang, K.; Kong, L.; Liu, J. Review of fluoride removal from water environment by adsorption. *J. Environ. Chem. Eng.* **2020**, *8*, 104516. [[CrossRef](#)]
22. Varalakshmi, V.; Karthik, V.; Selvakumar, P.; Muthumari, P. Investigation of Cephalexin Removal Using Biochar Derived from Nephelium lappaceum Seeds. *Glob. Nest J.* **2024**, *26*, 1–11.
23. Ben Amor, T.; Kassem, M.; Hajjaji, W.; Jamoussi, F.; Ben Amor, M.; Hafiane, A. Study of defluoridation of water using natural clay minerals. *Clays Clay Miner.* **2018**, *66*, 493–499. [[CrossRef](#)]
24. Zhang, S.; Lyu, Y.; Su, X.; Bian, Y.; Yu, B.; Zhang, Y. Removal of fluoride ion from groundwater by adsorption on lanthanum and aluminum loaded clay adsorbent. *Environ. Earth Sci.* **2016**, *75*, 401. [[CrossRef](#)]
25. Wang, R.; Luo, L.; Yang, Y.; Shu, L.; Jegatheesan, V.; Wang, H.; Yang, M. Preparation and characterization of mesoporous silica (Ms) supporting lanthanum carbonate (Ms-La) for the defluorination of aqueous solutions. *Desalin. Water Treat.* **2017**, *96*, 112–119. [[CrossRef](#)]
26. Zhang, L.; Tan, W.; Wang, R.; Yang, Y.; Yang, M.; Wang, H. The characterization of mesoporous silica (Ms) supporting cerium carbonate (Ms-Ce) and its adsorption performance for defluorination in aqueous solutions. *Desalin. Water Treat.* **2018**, *135*, 362–371. [[CrossRef](#)]
27. Wang, X.G.; Zhu, H.; Sun, T.S.; Liu, Y.B.; Han, T.; Lu, J.X.; Dai, H.L.; Zhai, L.Z. Synthesis and Study of an Efficient Metal-Organic Framework Adsorbent (MIL-96(Al)) for Fluoride Removal from Water. *J. Nanomater.* **2019**, *2019*, 3128179. [[CrossRef](#)]
28. Balarak, D.; Mostafapour, F.K.; Bazrafshan, E.; Mahvi, A.H. The equilibrium, kinetic, and thermodynamic parameters of the adsorption of the fluoride ion on to synthetic nano sodalite zeolite. *Fluoride* **2017**, *50*, 223–234.
29. Saucedo-Delgado, B.G.; De Haro-Del Rio, D.A.; González-Rodríguez, L.M.; Reynel-Ávila, H.E.; Mendoza-Castillo, D.I.; Bonilla-Petriciolet, A.; de la Rosa, J.R. Fluoride adsorption from aqueous solution using a protonated clinoptilolite and its modeling with artificial neural network-based equations. *J. Fluor. Chem.* **2017**, *204*, 98–106. [[CrossRef](#)]
30. He, J.; Zhang, K.; Wu, S.; Cai, X.; Chen, K.; Li, Y.; Sun, B.; Jia, Y.; Meng, F.; Jin, Z.; et al. Performance of novel hydroxyapatite nanowires in treatment of fluoride contaminated water. *J. Hazard. Mater.* **2016**, *303*, 119–130. [[CrossRef](#)]
31. Mehta, D.; Mondal, P.; Saharan, V.K.; George, S. Synthesis of hydroxyapatite nanorods for application in water defluoridation and optimization of process variables: Advantage of ultrasonication with precipitation method over conventional method. *Ultrason. Sonochem.* **2017**, *37*, 56–70. [[CrossRef](#)] [[PubMed](#)]
32. Jia, Y.; Zhu, B.S.; Jin, Z.; Sun, B.; Luo, T.; Yu, X.Y.; Kong, L.T.; Liu, J.H. Fluoride removal mechanism of bayerite/boehmite nanocomposites: Roles of the surface hydroxyl groups and the nitrate anions. *J. Colloid Interface Sci.* **2015**, *440*, 60–67. [[CrossRef](#)]

33. Zhang, S.; Lü, Y.; Lin, X.; Zhang, Y.; Su, X. Performance and mechanisms of fluoride removal from groundwater by lanthanum-aluminum-loaded hydrothermal palygorskite composite. *Chem. Res. Chin. Univ.* **2015**, *31*, 144–148. [[CrossRef](#)]
34. Zhu, B.S.; Jia, Y.; Jin, Z.; Sun, B.; Luo, T.; Yu, X.Y.; Kong, L.T.; Huang, X.J.; Liu, J.H. Controlled synthesis of natroalunite microtubes and spheres with excellent fluoride removal performance. *Chem. Eng. J.* **2015**, *271*, 240–251. [[CrossRef](#)]
35. Ali, I.; AlOthman, Z.A.; Sanagi, M.M. Green synthesis of iron nano-impregnated adsorbent for fast removal of fluoride from water. *J. Mol. Liq.* **2015**, *211*, 457–465. [[CrossRef](#)]
36. Zhang, C.; Li, Y.; Wang, T.J.; Jiang, Y.; Fok, J. Synthesis and properties of a high-capacity iron oxide adsorbent for fluoride removal from drinking water. *Appl. Surf. Sci.* **2017**, *425*, 272–281. [[CrossRef](#)]
37. Kumari, U.; Behera, S.K.; Meikap, B.C. A novel acid modified alumina adsorbent with enhanced defluoridation property: Kinetics, isotherm study and applicability on industrial wastewater. *J. Hazard. Mater.* **2019**, *365*, 868–882. [[CrossRef](#)]
38. Zhu, J.; Lin, X.; Wu, P.; Zhou, Q.; Luo, X. Fluoride removal from aqueous solution by Al (III)–Zr (IV) binary oxide adsorbent. *Appl. Surf. Sci.* **2015**, *357*, 91–100. [[CrossRef](#)]
39. Yu, Y.; Zhou, Z.; Ding, Z.; Zuo, M.; Cheng, J.; Jing, C. Simultaneous arsenic and fluoride removal using {201} TiO<sub>2</sub>–ZrO<sub>2</sub>: Fabrication, characterization, and mechanism. *J. Hazard. Mater.* **2019**, *377*, 267–273. [[CrossRef](#)]
40. Tao, W.; Zhong, H.; Pan, X.; Wang, P.; Wang, H.; Huang, L. Removal of fluoride from wastewater solution using Ce-ALOOH with oxalic acid as modification. *J. Hazard. Mater.* **2020**, *384*, 121373. [[CrossRef](#)]
41. Chi, Y.L.; Chen, Y.T.; Hu, C.L.; Wang, Y.S.; Liu, C. Preparation of Mg-Al-Ce triple-metal composites for fluoride removal from aqueous solutions. *J. Mol. Liq.* **2017**, *242*, 416–422. [[CrossRef](#)]
42. Wang, M.; Yu, X.L.; Yang, C.L.; Yang, X.Q.; Lin, M.Y.; Guan, L.T.; Ge, M.F. Removal of fluoride from aqueous solution by Mg-Al-Zr triple-metal composite. *Chem. Eng. J.* **2017**, *322*, 246–253. [[CrossRef](#)]
43. Yu, Y.; Yu, L.; Chen, J.P. Adsorption of fluoride by Fe-Mg-La triple-metal composite: Adsorbent preparation, illustration of performance and study of mechanisms. *Chem. Eng. J.* **2015**, *262*, 839–846. [[CrossRef](#)]
44. Cai, H.M.; Chen, G.J.; Peng, C.Y.; Xu, L.Y.; Zhu, X.H.; Zhang, Z.Z.; Dong, Y.Y.; Shang, G.Z.; Ke, F.; Gao, H.J.; et al. Enhanced removal of fluoride by tea waste supported hydrous aluminium oxide nanoparticles: Anionic polyacrylamide mediated aluminium assembly and adsorption mechanism. *RSC Adv.* **2015**, *5*, 29266–29275. [[CrossRef](#)]
45. El-Said, G.F.; El-Sadaawy, M.M.; Aly-Eldeen, M.A. Adsorption isotherms and kinetic studies for the defluoridation from aqueous solution using eco-friendly raw marine green algae, *Ulva lactuca*. *Environ. Monit. Assess.* **2018**, *190*, 14. [[CrossRef](#)]
46. Dehghani, M.H.; Farhang, M.; Alimohammadi, M.; Afsharnia, M.; McKay, G. Adsorptive removal of fluoride from water by activated carbon derived from CaCl<sub>2</sub>-modified *Crocus sativus* leaves: Equilibrium adsorption isotherms, optimization, and influence of anions. *Chem. Eng. Commun.* **2018**, *205*, 955–965. [[CrossRef](#)]
47. Kazi, T.G.; Brahman, K.D.; Baig, J.A.; Afridi, H.I. A new efficient indigenous material for simultaneous removal of fluoride and inorganic arsenic species from groundwater. *J. Hazard. Mater.* **2018**, *357*, 159–167. [[CrossRef](#)]
48. Manna, S.; Saha, P.; Roy, D.; Sen, R.; Adhikari, B. Defluoridation potential of jute fibers grafted with fatty acyl chain. *Appl. Surf. Sci.* **2015**, *356*, 30–38. [[CrossRef](#)]
49. Xu, L.Y.; Chen, G.J.; Peng, C.Y.; Qiao, H.H.; Ke, F.; Hou, R.Y.; Li, D.X.; Cai, H.M.; Wan, X.C. Adsorptive removal of fluoride from drinking water using porous starch loaded with common metal ions. *Carbohydr. Polym.* **2017**, *160*, 82–89. [[CrossRef](#)]
50. Sankararamkrishnan, N.; Srivastava, I.; Mishra, S. Studies on novel nano-bimetal doped cellulose nanofibers derived from agrowaste towards defluoridation. *Int. J. Biol. Macromol.* **2019**, *128*, 556–565. [[CrossRef](#)]
51. Kang, J.H.; Gou, X.Q.; Hu, Y.H.; Sun, W.; Liu, R.Q.; Gao, Z.Y.; Guan, Q.J. Efficient utilisation of flue gas desulfurization gypsum as a potential material for fluoride removal. *Sci Total Environ.* **2019**, *649*, 344–352. [[CrossRef](#)] [[PubMed](#)]
52. Raghav, S.; Kumar, D. Comparative kinetics and thermodynamic studies of fluoride adsorption by two novel synthesized biopolymer composites. *Carbohydr. Polym.* **2019**, *203*, 430–440. [[CrossRef](#)] [[PubMed](#)]
53. Wang, J.; Lin, X.Y.; Luo, X.G.; Yao, W.H. Preparation and characterization of the linked lanthanum carboxymethylcellulose microsphere adsorbent for removal of fluoride from aqueous solutions. *RSC Adv.* **2015**, *5*, 59273–59285. [[CrossRef](#)]
54. Chen, J.; Shu, C.J.; Wang, N.; Feng, J.T.; Ma, H.Y.; Yan, W. Adsorbent synthesis of polypyrrole/TiO<sub>2</sub> for effective fluoride removal from aqueous solution for drinking water purification: Adsorbent characterization and adsorption mechanism. *J. Colloid Interface Sci.* **2017**, *495*, 44–52. [[CrossRef](#)]
55. Sharma, P.; Sen, K.; Thakur, P.; Chauhan, M.; Chauhan, K. Spherically shaped pectin-g-poly(amidoxime)-Fe complex: A promising innovative pathway to tailor a new material in high amidoxime functionalization for fluoride adsorption. *Int. J. Biol. Macromol.* **2019**, *140*, 78–90. [[CrossRef](#)]
56. Rungrodnimitchai, S.; Kotatha, D. Chemically modified ground tire rubber as fluoride ions adsorbents. *Chem. Eng. J.* **2015**, *282*, 161–169. [[CrossRef](#)]
57. Phillips, D.H.; Sen Gupta, B.; Mukhopadhyay, S.; Sen Gupta, A.K. Arsenic and fluoride removal from contaminated drinking water with Haix-Fe-Zr and Haix-Zr resin beads. *J. Environ. Manag.* **2018**, *215*, 132–142. [[CrossRef](#)]
58. Batten, S.R.; Champness, N.R.; Chen, X.-M.; Garcia-Martinez, J.; Kitagawa, S.; Ohrstrom, L.; O’Keeffe, M.; Suh, M.P.; Reedijk, J. Terminology of metal-organic frameworks and coordination polymers (IUPAC Recommendations 2013). *Pure Appl. Chem* **2013**, *85*, 1715–1724. [[CrossRef](#)]
59. Banerjee, D.; Cairns, A.J.; Liu, J.; Motkuri, R.K.; Nune, S.K.; Fernandez, C.A.; Krishna, R.; Strachan, D.M.; Thallapally, P.K. Potential of Metal-Organic Frameworks for Separation of Xenon and Krypton. *Acc. Chem. Res.* **2015**, *48*, 211–219. [[CrossRef](#)]



60. Karmakar, S.; Dechnik, J.; Janiak, C.; De, S. Aluminium fumarate metal-organic framework: A super adsorbent for fluoride from water. *J. Hazard. Mater.* **2016**, *303*, 10–20. [[CrossRef](#)]
61. Ke, F.; Luo, G.; Chen, P.R.; Jiang, J.; Yuan, Q.Y.; Cai, H.M.; Peng, C.Y.; Wan, X.C. Porous metal-organic frameworks adsorbents as a potential platform for defluoridation of water. *J. Porous Mater.* **2016**, *23*, 1065–1073. [[CrossRef](#)]
62. Zhao, C.Q.; Cui, Y.W.; Fang, F.; Ryu, S.O.; Huang, J.R. Synthesis of a Novel Ce-bpdc for the Effective Removal of Fluoride from Aqueous Solution. *Adv. Cond. Matter Phys.* **2017**, 8305765. [[CrossRef](#)]
63. Ma, A.Q.; Ke, F.; Jiang, J.; Yuan, Q.Y.; Luo, Z.D.; Liu, J.Q.; Kumar, A. Two lanthanide-based metal-organic frameworks for highly efficient adsorption and removal of fluoride ions from water. *CrystEngComm* **2017**, *19*, 2172–2177. [[CrossRef](#)]
64. Huang, P.P.; Cao, C.Y.; Wei, F.; Sun, Y.B.; Song, W.G. MgAl layered double hydroxides with chloride and carbonate ions as interlayer anions for removal of arsenic and fluoride ions in water. *RSC Adv.* **2015**, *5*, 10412–10417. [[CrossRef](#)]
65. Liu, J.M.; Yue, X.P.; Lu, X.Y.; Guo, Y. Uptake Fluoride from Water by Starch Stabilized Layered Double Hydroxides. *Water* **2018**, *10*, 745. [[CrossRef](#)]
66. Ghosal, P.S.; Gupta, A.K. An insight into thermodynamics of adsorptive removal of fluoride by calcined Ca-Al-(NO<sub>3</sub>) layered double hydroxide. *RSC Adv.* **2015**, *5*, 105889–105900. [[CrossRef](#)]
67. Dore, E.; Frau, F. Calcined and uncalcined carbonate layered double hydroxides for possible water defluoridation in rural communities of the East African Rift Valley. *J. Water Process Eng.* **2019**, *31*, 100855. [[CrossRef](#)]
68. Hafiz, M.; Hawari, A.H.; Alfahel, R.; Hassan, M.K.; Altaee, A. Comparison of nanofiltration with reverse osmosis in reclaiming tertiary treated municipal wastewater for irrigation purposes. *Membranes* **2021**, *11*, 32. [[CrossRef](#)]
69. Jin, T.; Peydayesh, M.; Mezzenga, R. Membrane-based technologies for per- and poly-fluoroalkyl substances (PFASs) removal from water: Removal mechanisms, applications, challenges, and perspectives. *Environ. Int.* **2021**, *157*, 106876. [[CrossRef](#)]
70. Marzak, P.; Yun, J.; Dorsel, A.; Kriele, A.; Gilles, R.; Schneider, O.; Bandarenka, A.S. Electrodeposited Na<sub>2</sub>Ni[Fe(CN)<sub>6</sub>] thin-film cathodes exposed to simulated aqueous Na-ion battery conditions. *J. Phys. Chem.* **2018**, *122*, 8760–8768. [[CrossRef](#)]
71. Jain, H.; Garg, M.C. Fabrication of polymeric nanocomposite forward osmosis membranes for water desalination—A review. *Environ. Technol. Innov.* **2021**, *23*, 101561. [[CrossRef](#)]
72. Al-Aani, S.; Mustafa, T.N.; Hilal, N. Ultrafiltration membranes for wastewater and water process engineering: A comprehensive statistical review over the past decade. *J. Water Process Eng.* **2018**, *35*, 101241. [[CrossRef](#)]
73. Dahiya, S.; Singh, A.; Mishra, B.K. Capacitive deionized hybrid systems for wastewater treatment and desalination: A review on synergistic effects, mechanisms, and challenges. *Chem. Eng. J.* **2020**, *417*, 128129. [[CrossRef](#)]
74. Chekli, L.; Phuntsho, S.; Kim, J.E.; Kim, J.; Choi, J.Y.; Choi, J.S.; Kim, S.; Kim, J.H.; Hong, S.; Sohn, J.; et al. A comprehensive review of hybrid forward osmosis systems: Performance, applications and future prospects. *J. Membr. Sci.* **2015**, *497*, 430–449. [[CrossRef](#)]
75. Ansari, A.J.; Hai, F.I.; Price, W.E.; Drewes, J.E.; Nghiem, L.D. Forward osmosis as a platform for resource recovery from municipal wastewater—A critical assessment of the literature. *J. Membr. Sci.* **2017**, *529*, 195–206. [[CrossRef](#)]
76. Chung, T.; Li, X.; Ong, R.C.; Ge, Q.; Wang, H.; Han, G. Emerging forward osmosis (FO) technologies and challenges ahead for clean water and clean energy applications. *Curr. Opin. Chem. Eng.* **2012**, *1*, 246–257. [[CrossRef](#)]
77. Pal, M.; Chakraborty, S.; Pal, P. Purifying fluoride-contaminated water by a novel forward osmosis design with enhanced flux under reduced concentration polarization. *Environ. Sci. Pollut. Res.* **2015**, *22*, 11401–11411. [[CrossRef](#)]
78. Cath, T.Y.; Childress, A.E.; Elimelech, M. Forward osmosis: Principles, applications, and recent developments. *J. Membr. Sci.* **2006**, *281*, 70–87. [[CrossRef](#)]
79. Shen, J.; Schäfer, A. Removal of fluoride and uranium by nanofiltration and reverse osmosis: A review. *Chemosphere* **2014**, *117*, 679–691. [[CrossRef](#)]
80. He, J.; Cai, X.; Chen, K.; Li, Y.; Zhang, K.; Jin, Z.; Meng, F.; Liu, N.; Wang, X.; Kong, L.; et al. Performance of a novel zirconium metal-organic frameworks adsorption membrane in fluoride removal. *J. Colloid Interface Sci.* **2016**, *484*, 162–172. [[CrossRef](#)]
81. Strathmann, H. Ion-Exchange Membrane Processes in Water Treatment. *Sustain. Sci. Eng.* **2010**, *2*, 141–199.
82. Othman, N.H.; Alias, N.H.; Fuzil, N.S.; Marpani, F.; Shahrudin, M.Z.; Chew, C.M.; David Ng, K.M.; Lau, W.J.; Ismail, A.F. A review on the use of membrane technology systems in developing countries. *Membranes* **2021**, *12*, 30. [[CrossRef](#)] [[PubMed](#)]
83. Mena VFBetancor-Abreu AGonzález SDelgado SSouto, R.M.; Santana, J.J. Fluoride removal from natural volcanic underground water by an electrocoagulation process: Parametric and cost evaluations. *J. Environ. Manag.* **2019**, *246*, 472–483.
84. Pulkka, S.; Martikainen, M.; Bhatnagar, A.; Sillanpää, M. Electrochemical methods for the removal of anionic contaminants from water—A review. *Sep. Purif. Technol.* **2014**, *132*, 252–271. [[CrossRef](#)]
85. Brillas, E.; Martínez-Huitle, C.A. Decontamination of wastewaters containing synthetic organic dyes by electrochemical methods: An updated review. *Appl. Catal. B* **2015**, *166–167*, 603–643. [[CrossRef](#)]
86. Nidheesh, P.V.; Singh, T.S.A. Arsenic removal by electrocoagulation process: Recent trends and removal mechanisms. *Chemosphere* **2017**, *181*, 418–433. [[CrossRef](#)]
87. Amarasooriya, T.; Kawakami, T. Electrolysis removal of fluoride by magnesium ion-assisted sacrificial iron electrode and the effect of coexisting ions. *J. Environ. Manag.* **2019**, *7*, 103084. [[CrossRef](#)]
88. Hakizimana, J.N.; Gourich, B.; Chafi, M.; Stiriba, Y.; Vial, C.; Drogui, P.; Naja, J. Electrocoagulation process in water treatment: A review of electrocoagulation modeling approaches. *Desalination* **2017**, *404*, 1–21. [[CrossRef](#)]
89. Sandoval, M.A.; Fuentes, R.; Thiam, A.; Salazar, R. Arsenic and fluoride removal by electrocoagulation process: A general review. *Sci. Total Environ.* **2020**, *753*, 142108. [[CrossRef](#)]

90. López-Guzmán, M.; Alarcón-Herrera, M.T.; Irigoyen-Campuzano, J.R.; Torres-Castañón, L.A.; Reynoso-Cuevas, L. Simultaneous removal of fluoride and arsenic from well water by electrocoagulation. *Sci. Total Environ.* **2019**, *678*, 181–187. [[CrossRef](#)]
91. Kim, K.J.; Baek, K.; Ji, S.; Cheong, Y.; Yim, G.; Jang, A. Study on electrocoagulation parameters (current density, pH, and electrode distance) for removal of fluoride from groundwater. *Environ. Earth Sci* **2016**, *75*, 45. [[CrossRef](#)]
92. Brown, T.C.; Mahat, V.; Ramirez, J.A. Adaptation to future water shortages in the United States caused by population growth and climate change. *Earth's Future* **2019**, *7*, 219–234. [[CrossRef](#)]
93. De Oliveira, J.T.; de Carvalho Costa, L.R.; Nunes, K.G.P.; Jurado-Davila, V.; de Oliveira, R.A.; Carissimi, E.; Féris, L.A. Adsorptive processes applied to the defluorination of groundwater for human consumption. *Clean. Chem. Eng.* **2024**, *10*, 100131. [[CrossRef](#)]
94. Dhakal, N.; Salinas-Rodriguez, S.G.; Hamdani, J.; Abushaban, A.; Sawalha, H.; Schippers, J.C.; Kennedy, M.D. Is desalination a solution to freshwater scarcity in developing countries? *Membranes* **2022**, *12*, 381. [[CrossRef](#)]
95. Ankita, A. A brief review of micellar enhanced ultrafiltration (MEUF) techniques for treatment of wastewater in India. *J. Water Resour. Eng. Manag.* **2020**, *1*, 14–30. [[CrossRef](#)]

**Disclaimer/Publisher's Note:** The statements, opinions and data contained in all publications are solely those of the individual author(s) and contributor(s) and not of MDPI and/or the editor(s). MDPI and/or the editor(s) disclaim responsibility for any injury to people or property resulting from any ideas, methods, instructions or products referred to in the content.